CORE
Metadata, citation and similar papers at core.ac.uk
Provided by NASA Technical Reports Server

N71 34237

Report No. F-71-1

AN EXPERIMENTAL INVESTIGATION OF THE TURBULENT BOUNDARY LAYER UNDERGOING BOTH ADVERSE PRESSURE GRADIENT AND CROSS FLOW ALONG A PLANE OF SYMMETRY

by

Victor Zakkay

Wladimiro Calarese

C. R. Wang

Department of Aeronautics and Astronautics

CASE FILE COPY

Prepared for The

Office of University Affairs

National Aeronautics and Space Administration

under Grant

NGL-33-016-067

February 1971

New York University
School of Engineering and Science
University Heights, New York, N.Y. 10453

Report No. F-71-1

NEW YORK UNIVERSITY
New York, New York

AN EXPERIMENTAL INVESTIGATION OF THE TURBULENT BOUNDARY LAYER UNDERGOING BOTH ADVERSE PRESSURE GRADIENT AND CROSS FLOW ALONG A PLANE OF SYMMETRY

by

Victor Zakkay
Professor of Aeronautics and Astronautics

Wladimiro Calarese
Assistant Research Scientist

and

C. R. Wang
Research Assistant

Department of Aeronautics and Astronautics

Prepared for The Office of University Affairs
National Aeronautics and Space Administration
under Research Grant NGL-33-016-067

February 1971

AN EXPERIMENTAL INVESTIGATION OF THE TURBULENT BOUNDARY LAYER UNDERGOING BOTH ADVERSE PRESSURE GRADIENT & CROSS FLOW ALONG A PLANE OF SYMMETRY*

by

Victor Zakkay†, Wladimiro Calarese††, C.R. Wang†††

ABSTRACT

Experimental data have been obtained for a compressible turbulent boundary layer in adverse pressure gradient with and without favorable cross flow along a plane of symmetry of a flared surface. The experiments were performed at Mach Number 6 and Reynolds Number up to 4.4×10^7/ft. The compression over the flared surface was of the order of 50. Transition was achieved naturally well ahead of the compression region and the cross flow was established by placing on the compression surface two lateral plates. Boundary layer profiles of static pressure, pitot tube pressure, stagnation temperature, and heat transfer rates were measured. Measurements were taken on the windward side of the surface. The presence of the cross flow alters significantly the value of the profiles. Heat transfer rates are in good agreement with theoretical values obtained by the flat-plate reference enthalpy method. A second part will follow where the

*This report was prepared under the following Grants, NGL-33-016-067 and NGR-33-016-161.

†Professor of Aeronautics and Astronautics, New York University
††Assistant Research Scientist, New York University
†††Research Assistant, New York University

present data will be used to calculate the Mach Number and velocity profiles, together with the boundary layer parameters.

NOMENCLATURE

c_f	skin friction coefficient
p	pressure
q_w	heat transfer rate
s	streamwise distance measured from beginning of flare
T	temperature
u	velocity in the streamwise direction
w	velocity in the peripheral direction
w^*	velocity ratio $\frac{w}{u_e}$
x	axial direction
y	direction normal to the body axis
δ	boundary layer thickness
η	local angle between the axis direction and the body surface
φ	peripheral direction

Subscripts

0	initial conditions at the beginning of the compression flare
1	static
2	behind normal shock
e	edge of boundary layer
t	stagnation conditions,
∞	free stream conditions

INTRODUCTION

Present interest in three-dimensional hypersonic turbulent boundary layers over inlets of air breathing propulsion systems has stimulated the present investigation. The effect of cross flow on a boundary layer subject to a large adverse pressure gradient is of utmost importance in the determination of the overall performance of the system and also in order to establish the upper limit on the maximum pressure rise without separating the flow within the inlet. Some investigators (Refs. 1-4) have presented detailed pressure measurements on three-dimensional boundary layers in absence of adverse pressure gradients, and others (Refs. 2-3-5) have confined themselves to measurements of boundary layers on axisymmetric bodies at zero angle of attack. The present data, instead, have been obtained for the case of both adverse pressure gradient and favorable cross flow. Measurements without cross flow have been taken for comparison. In spite of the fact that an adverse cross flow, as the one that results from the walls of the inlet, actually determines the upper criteria for separation, the measurements refer to the favorable cross flow condition at the meridian plane of an axisymmetric body.

The comparison of the pressure profiles with and without cross flow in the longitudinal direction shows that the cross flow relieves the pressure distribution along the body surface and, therefore, delays separation. The pressure variation in the peripheral direction increases considerably along the compression surface due to the adverse pressure gradient.

Total temperature and heat transfer profiles have been compared with theories and previous experimental results at zero angle of attack.

EXPERIMENTAL APPARATUS

All tests were conducted in the New York University blowdown-type tunnel equipped with a Mach 6 axially symmetric contoured nozzle. The test section is 1 ft. in diameter and consists of a uniform flow 9 inches in diameter and 3 ft. in length. The tunnel stagnation temperature was approximately 800^{o}R for all the tests, and the stagnation pressure varied between 1800 psia and 2000 psia. The model consisted of a streamlined cylindrical forebody generated from one of the nozzle streamlines starting in the settling chamber of the nozzle. A right circular cylinder 14.91 inches long and 4.62 inches in diameter was connected at the terminal part of the forebody. To this cylinder a compression flare 6.3 inches in length, described by a fourth order polynomial, was connected. Its maximum turning angle was 44^{o} (Figs. 1-3). The overall axial length of the model, from the nozzle throat to the test section, was 77 inches long. The model was made of 304 stainless steel and polish to high finish. It was placed at zero angle of attack and part of the tests were performed in the presence of an adverse pressure gradient only. Subsequently, two lateral curved plates were symmetrically placed on the sides of the model so to create an expansion in the peripheral direction and establish a favorable cross flow on the windward side of the flare, in addition to the adverse pressure gradient. The compression flare was equipped with 78 pressure taps, 0.02 inches in diameter drilled normal to the surface and distributed on the upper surface, in order to obtain the longitudinal as well as the peripheral pressure distribution. The flare was also equipped with chromel-alumel thermocouples to measure wall temperatures and transient heat transfer rates. In order to obtain measurements of static and pitot tube pressures,

single probes were used at different stations of the compression flare along the plane of symmetry. An unshielded, open-tip chromel-alumel thermocouple was used to measure the stagnation temperature throughout the boundary layer.

EXPERIMENTAL RESULTS

The flow field of the upper flare compression region, as seen in Schlieren photographs is shown in Fig. 4. Fig. 5 shows the surface pressure distribution on the flare with and without cross flow and the distribution obtained by Hoydysh and Zakkay (Ref. 2).

The static pressure profiles, obtained at various stations of the compression flare are plotted in Figs. 6 to 13, and the pitot pressure profiles in Figs. 14 to 21. These profiles refer to both cases with and without cross flow. It is seen that the cross flow relieves the pressure distribution along the compression flare, acting as suction and therefore reduces the growth of the boundary layer parameters, delaying separation on the windward side of the flare.

The experimental total temperature profiles are plotted in Figs. 22 to 29 and compared to the profiles obtained by using the Crocco relation. It is seen that the Crocco relation gives a fairly good approximation of the total temperature variation throughout the boundary layer.

Figs. 30 and 31 show the pressure distribution along the peripheral direction, at different stations, and the variation of the parameter $\frac{1}{pe}\frac{\partial^2 pe}{\partial \varphi^2}$, at the meridian plane, in the longitudinal direction. The substantial variation of the peripheral pressure distribution along the longitudinal direction is due to the presence of a large adverse pressure gradient on the compression flare. Since the magnitude of the cross flow is directly proportional to the parameter $\frac{1}{pe}\frac{\partial^2 pe}{\partial \varphi^2}$, it increases continuously with the compression surface length.

Fig. 32 compares the experimental value of the heat transfer for the case without cross flow to the flat plate reference enthalpy method and to Zakkay and Calarese theory (Ref. 6). The agreement is considered good downstream of the compression flare.

CONCLUSION

Experimental measurements of pressure, temperature and heat transfer have been taken over the meridian plane of a flared surface placed in a Mach 6 hypersonic stream in presence of an adverse pressure gradient and favorable cross flow. It has been concluded that the profiles are reduced by the cross flow effect and that boundary layer separation over the windward side of the compression surface is therefore delayed. The magnitude of the cross flow increases with increasing surface length, due to the presence of the adverse pressure gradient.

The cross flow effect should, therefore, be taken into consideration when boundary layer parameters, as displacement and momentum thickness, are to be predicted.

The present data will be used in the second part of this work to obtain accurate experimental values of all the boundary layer parameters at the meridian plane of the model.

REFERENCES

1) Braun, W.H., 1959, "Turbulent Boundary Layer on a Yawed Cone in a Supersonic Stream," NACA TN 4208.

2) Hoydysh, W.G. and Zakkay, V., "An Experimental Investigation of Hypersonic Turbulent Boundary Layers in Adverse Pressure Gradient," AIAA J. 4, Jan. 1969, p. 105.

3) McLafferty, G.H. and Barber, R.E., 1962 "The Effect of Adverse Pressure Gradients on the Characteristics of Turbulent Boundary Layers in Supersonic Streams," J. Aerospace Sci., 2, 1-11.

4) Rainbird, W.J., 1968, "Turbulent Boundary Layer Growth and Separation on a Yawed Cone," AIAA J., 3, 2410.

5) Stroud, J.F. and Miller, L.D., 1967, "An Experimental and Analytical Investigation of Hypersonic Inlet Boundary Layers," Technical Report, AFFDL TR-65-123.

6) Zakkay, V. and Calarese, W., "Cross Flow Effects on Compressible Turbulent Boundary Layer Over Bodies of Revolution," Israel Journal of Technology, Vol. 8, No. 1-2, 1970, p. 127.

LIST OF FIGURES

FIGURE

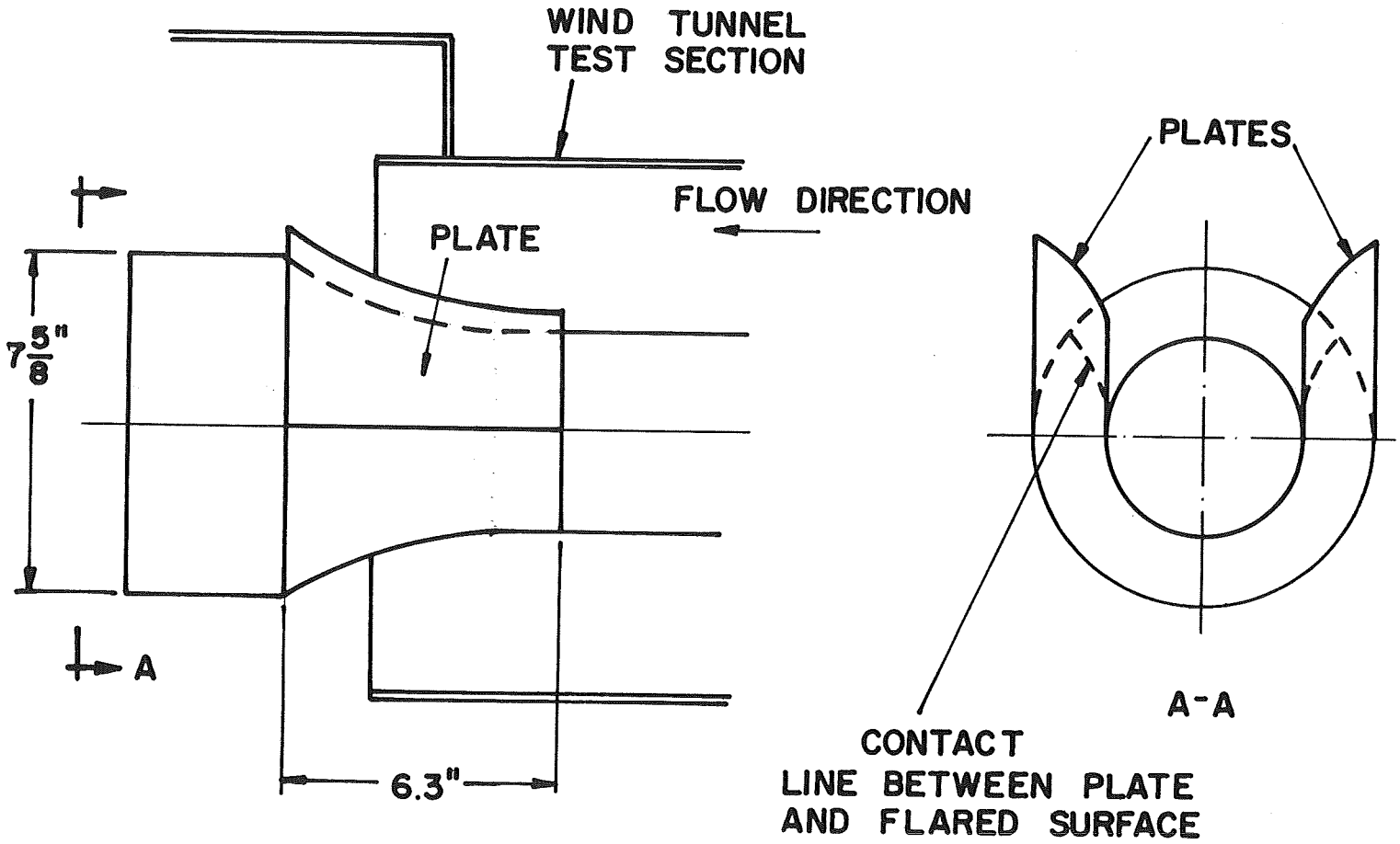

Fig. 1 View of Flared Surface with Lateral Plates

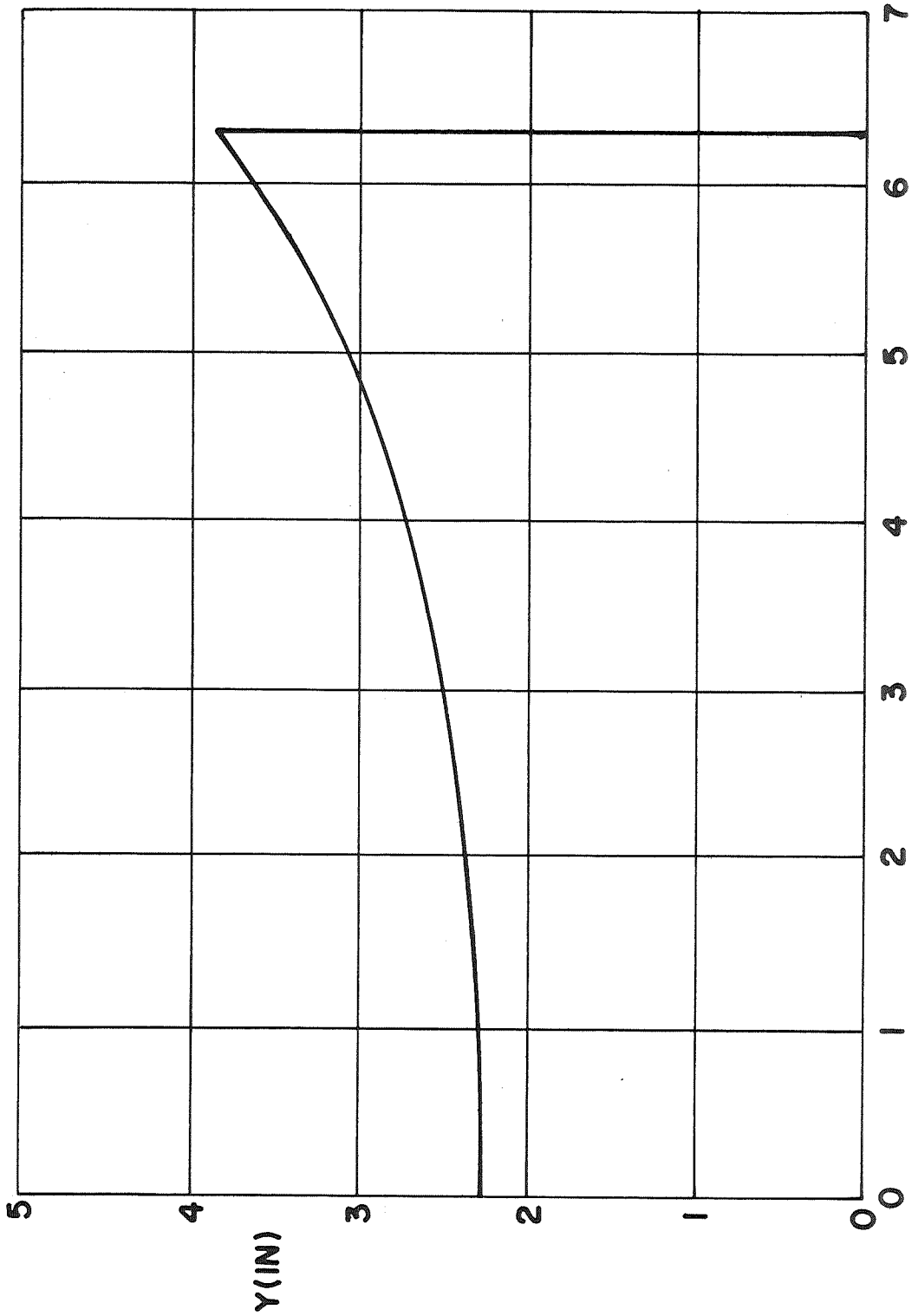

Fig. 2 Side View of Flared Surface without Lateral Plates

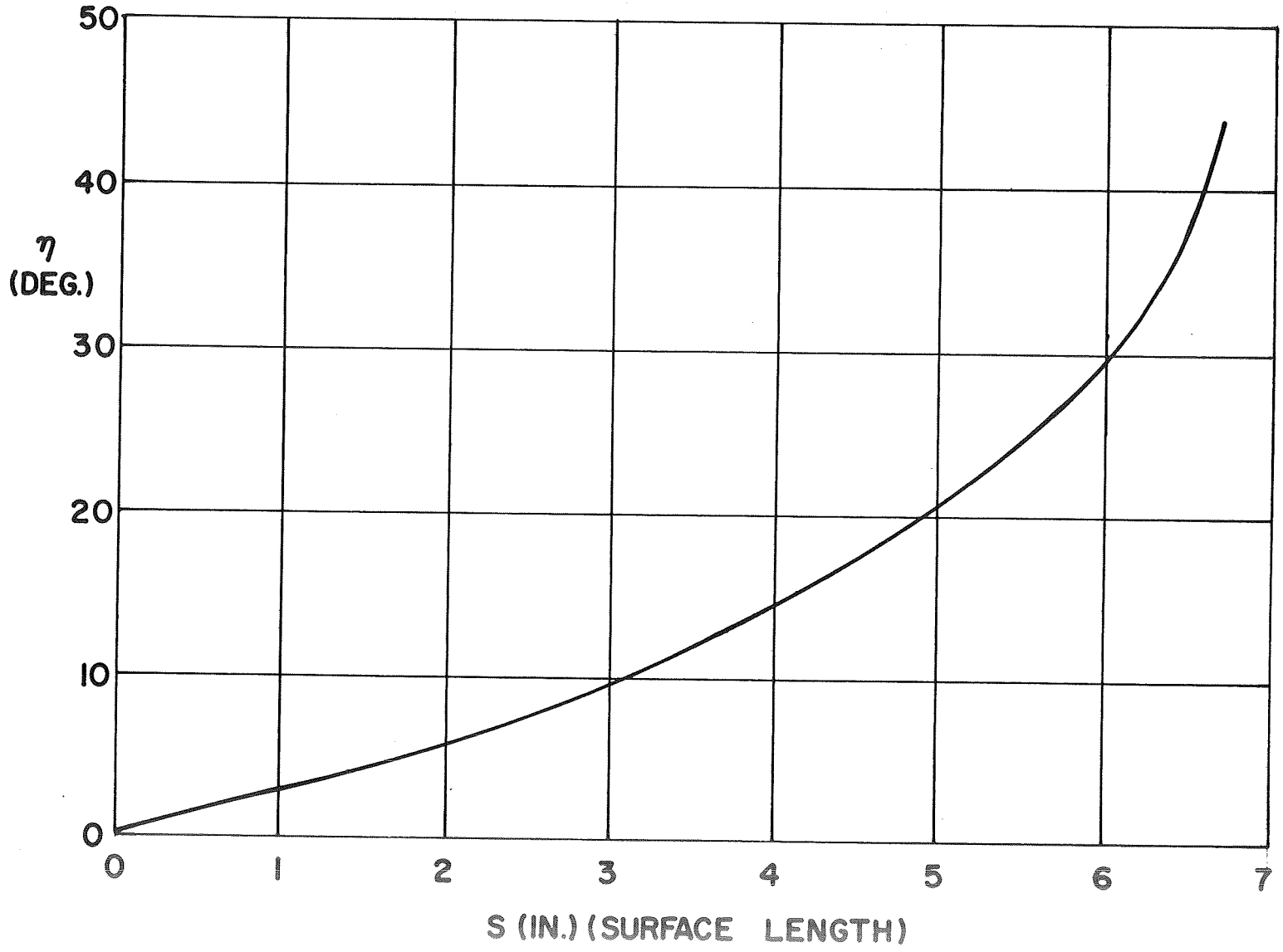

Fig. 3 Relation Between Local Surface Angle and Surface Length

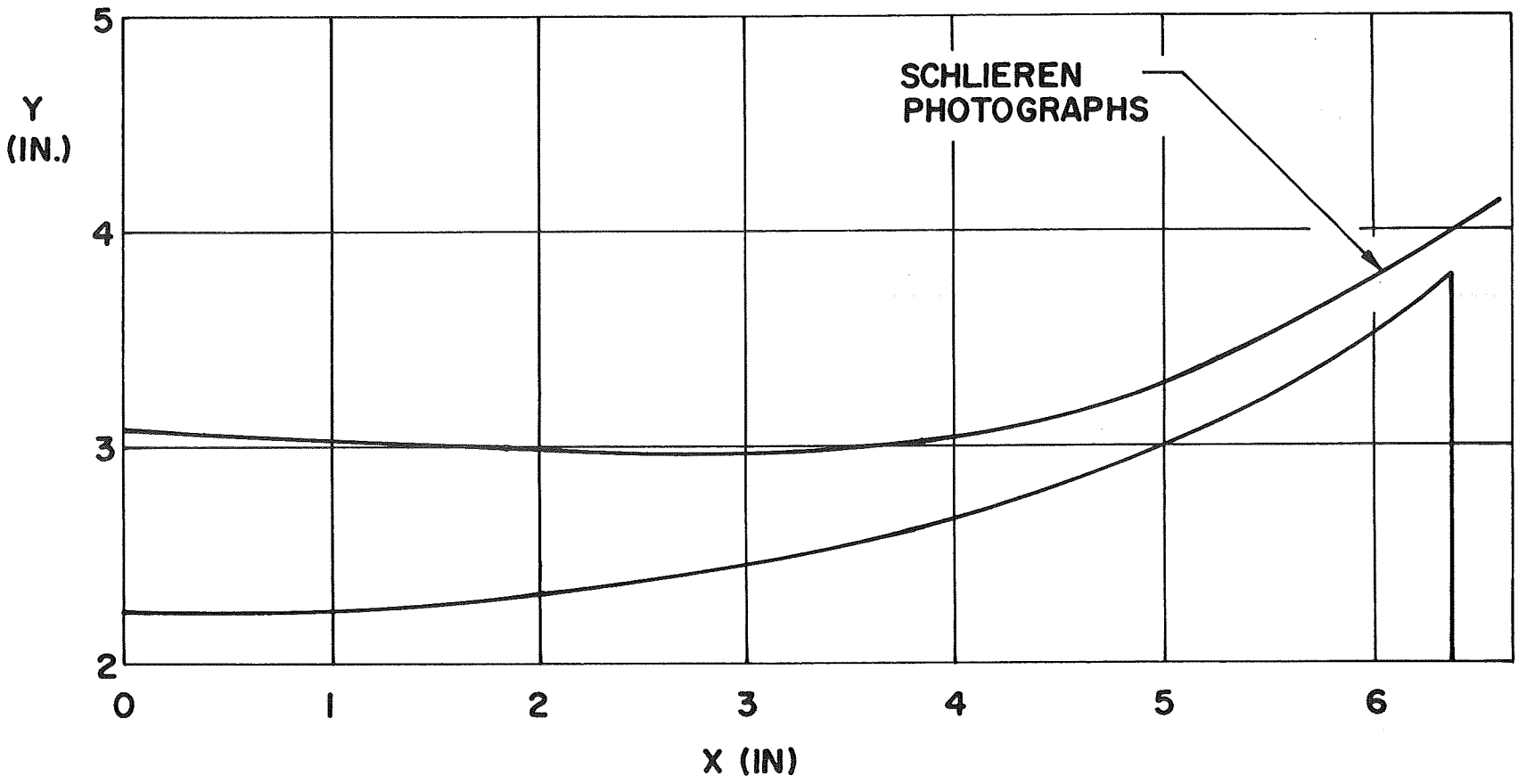

Fig. 4 Flow Field Compression Region as Seen in Schlieren Photographs

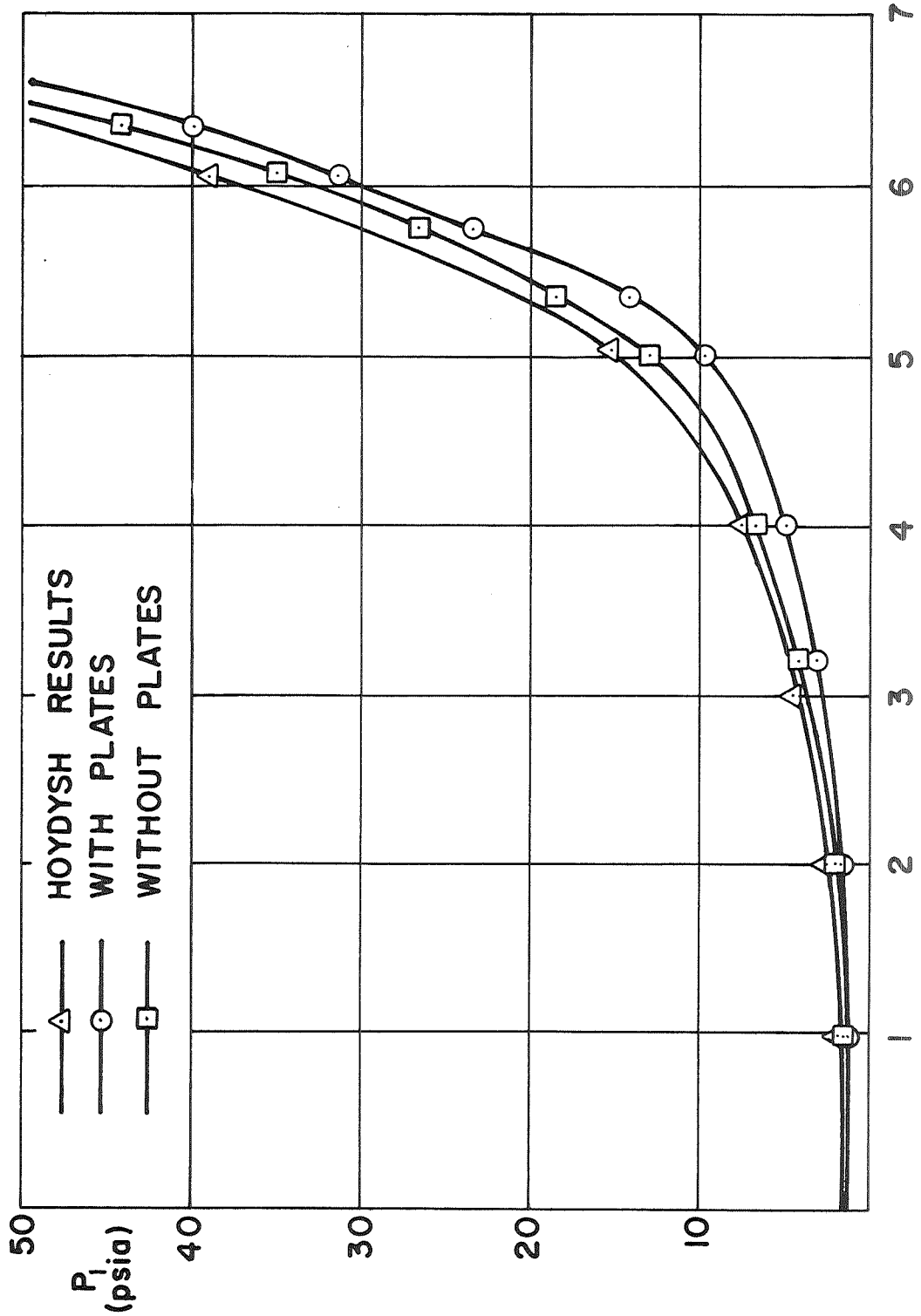

Fig. 5 Wall Pressure Distribution on Flared Surface

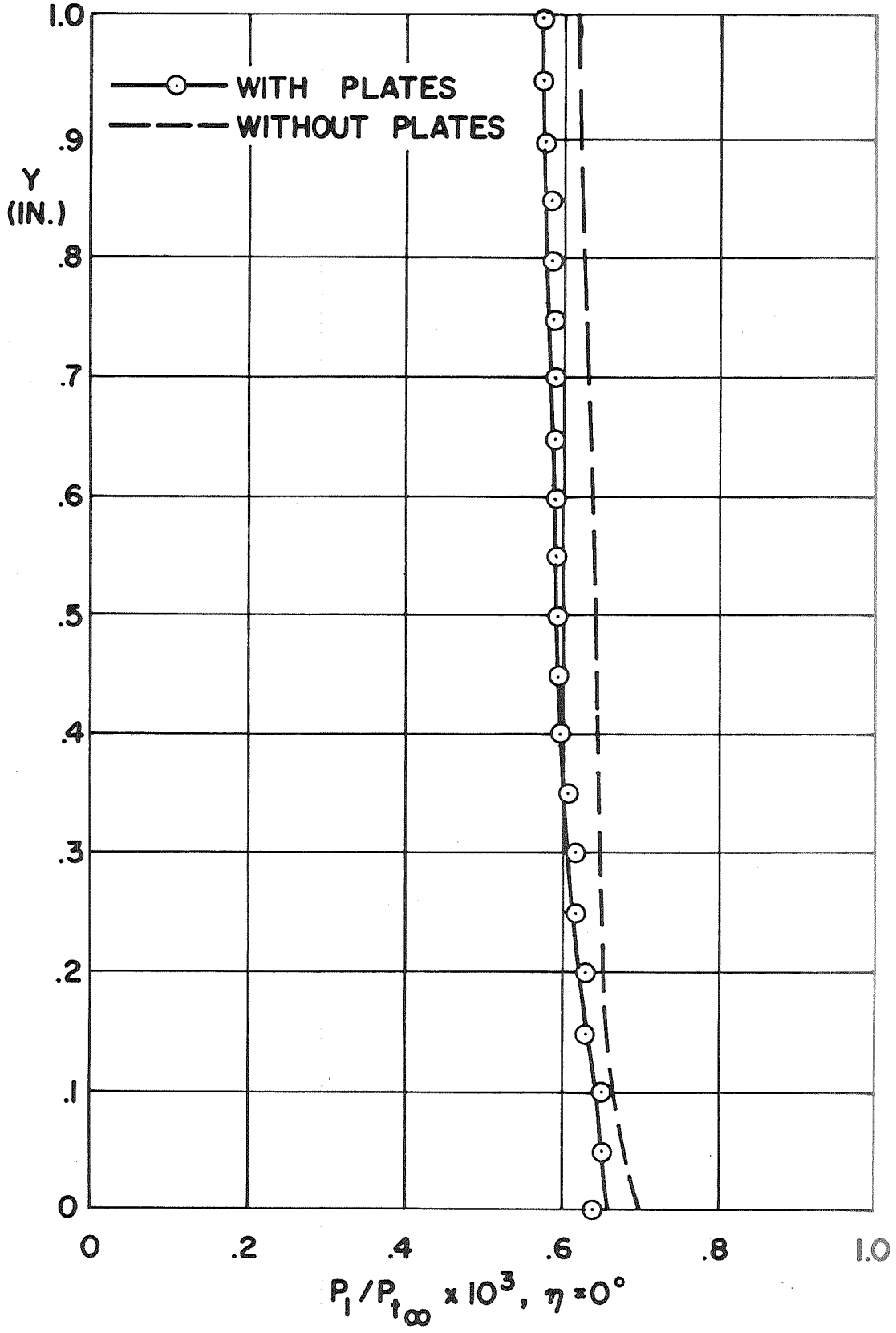

Fig. 6 Static Pressure Profile at $\eta = 0^{\circ}$

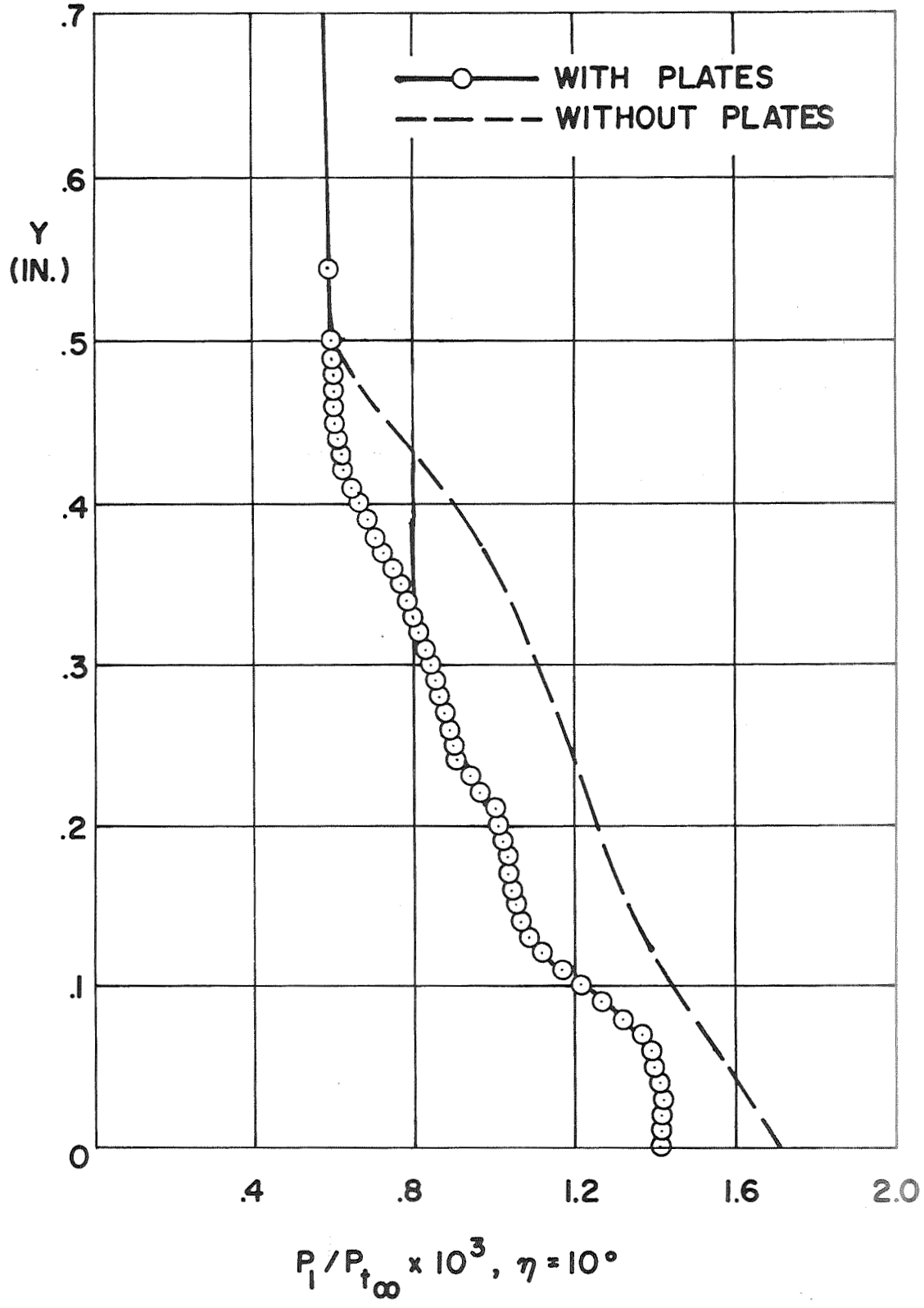

Fig. 7 Static Pressure Profile at $\eta = 10^{\circ}$

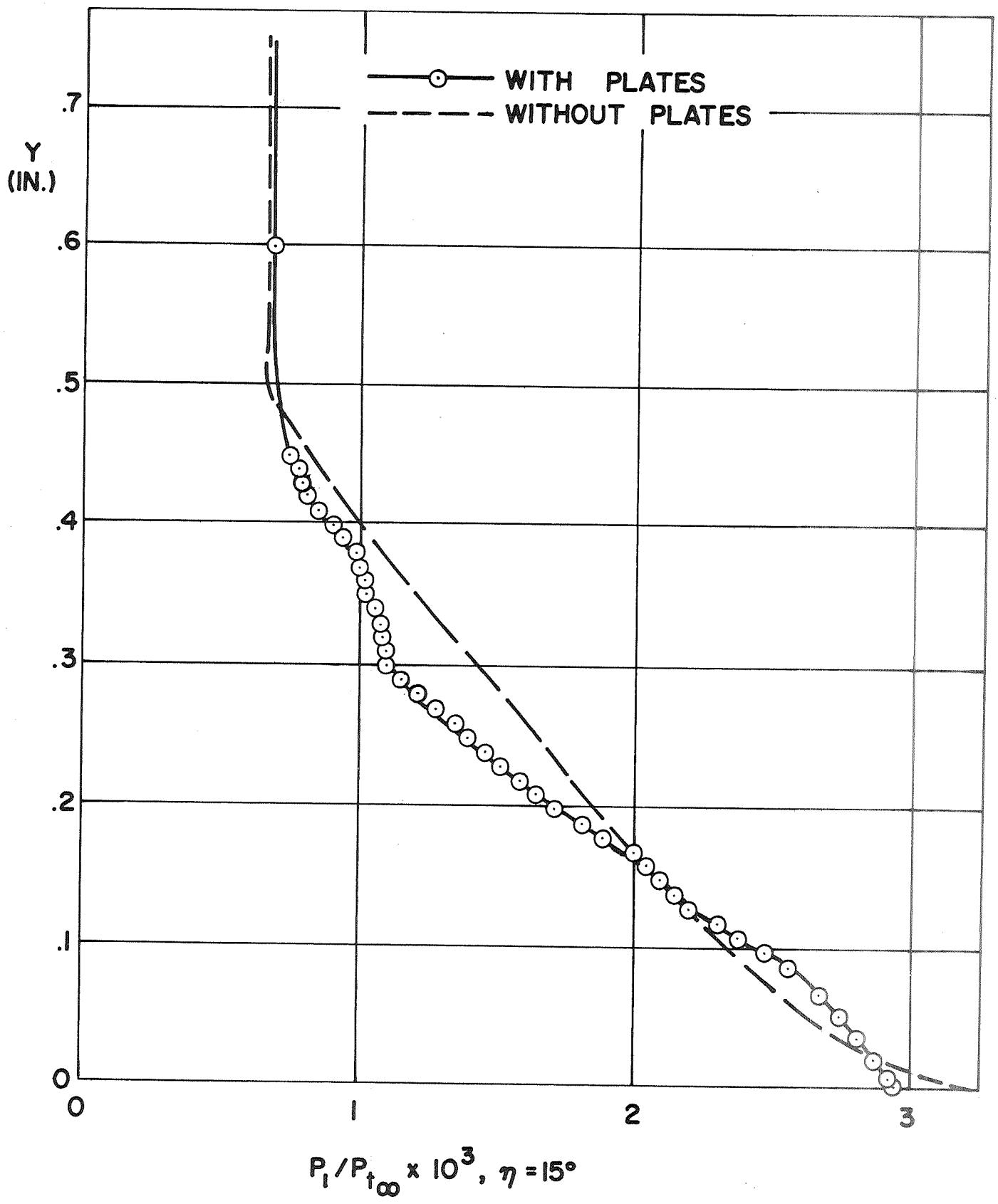

Fig. 8 Static Pressure Profile at $\eta = 15^{\circ}$

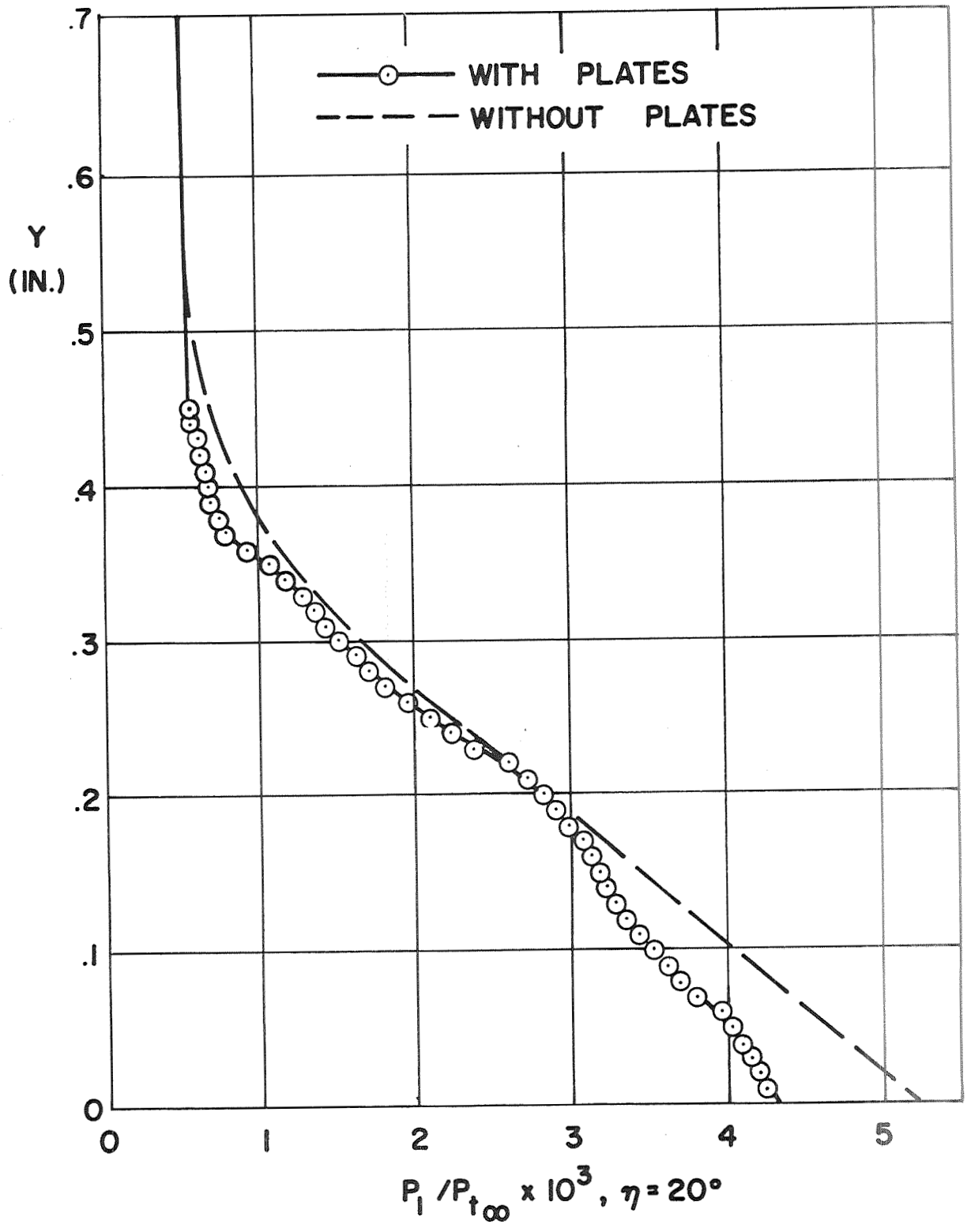

Fig. 9 Static Pressure Profile at $\eta = 20^{\circ}$

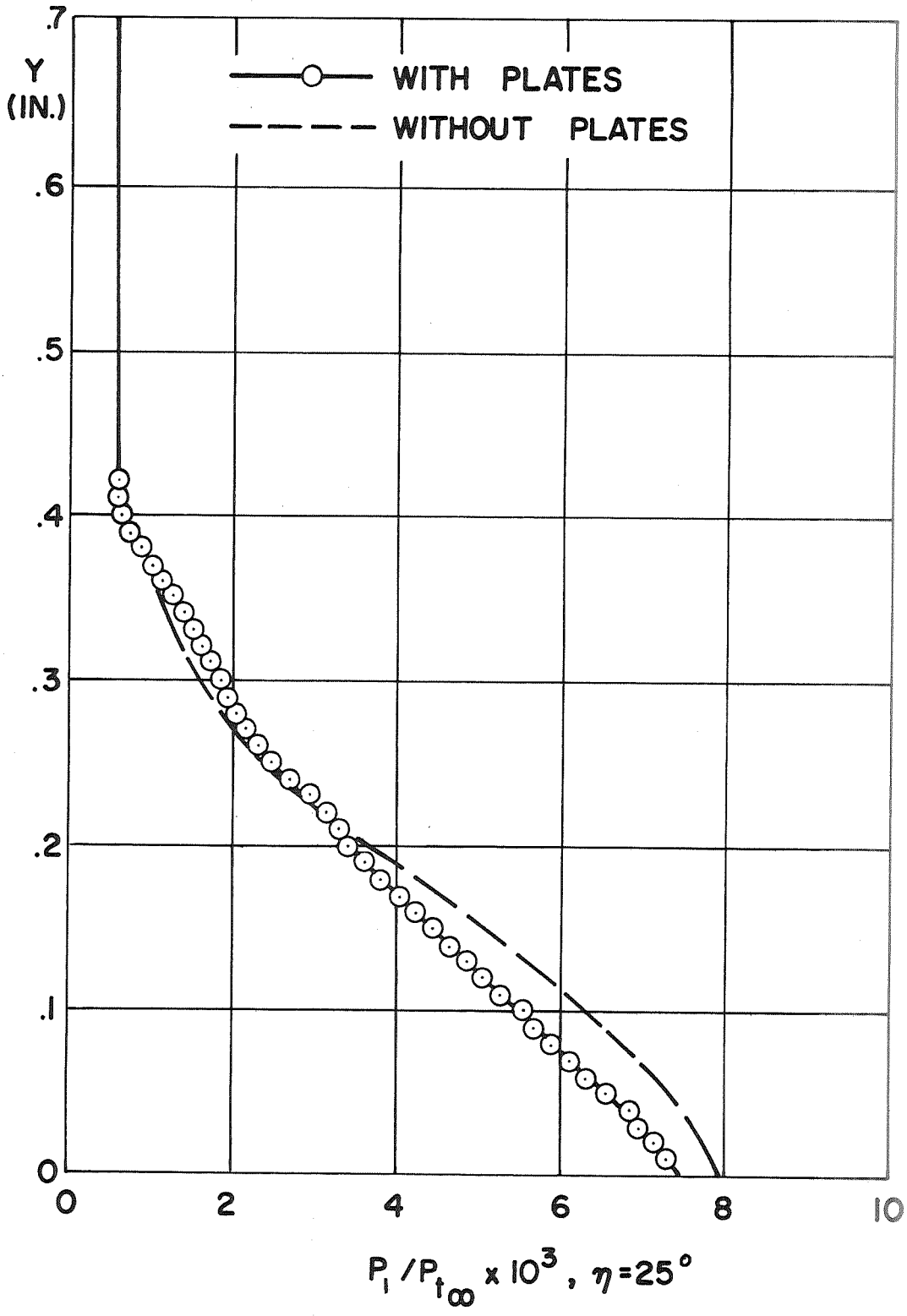

Fig. 10 Static Pressure Profile at $\eta = 25^{\circ}$

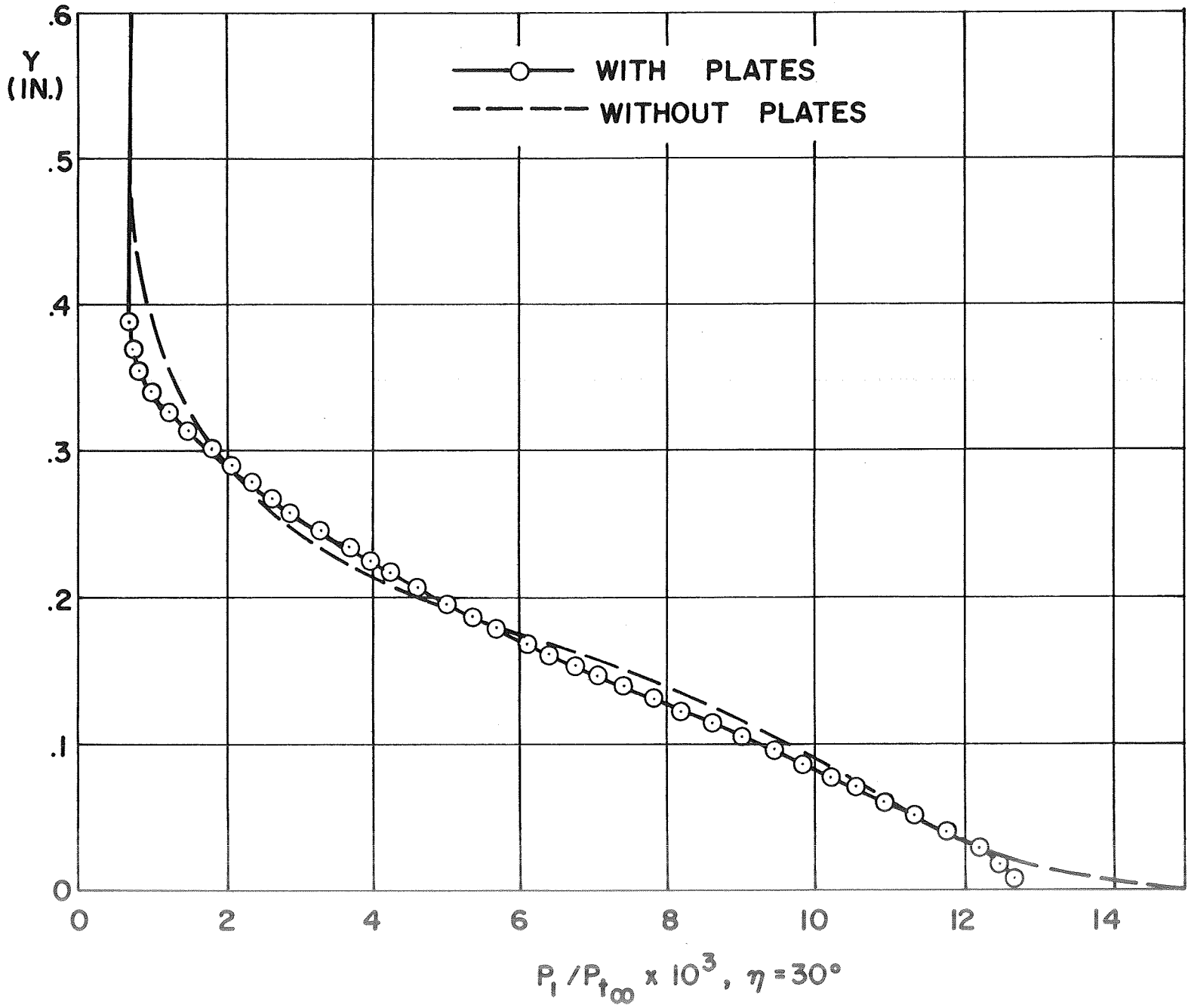

Fig. 11 Static Pressure Profile at $\eta = 30^{\circ}$

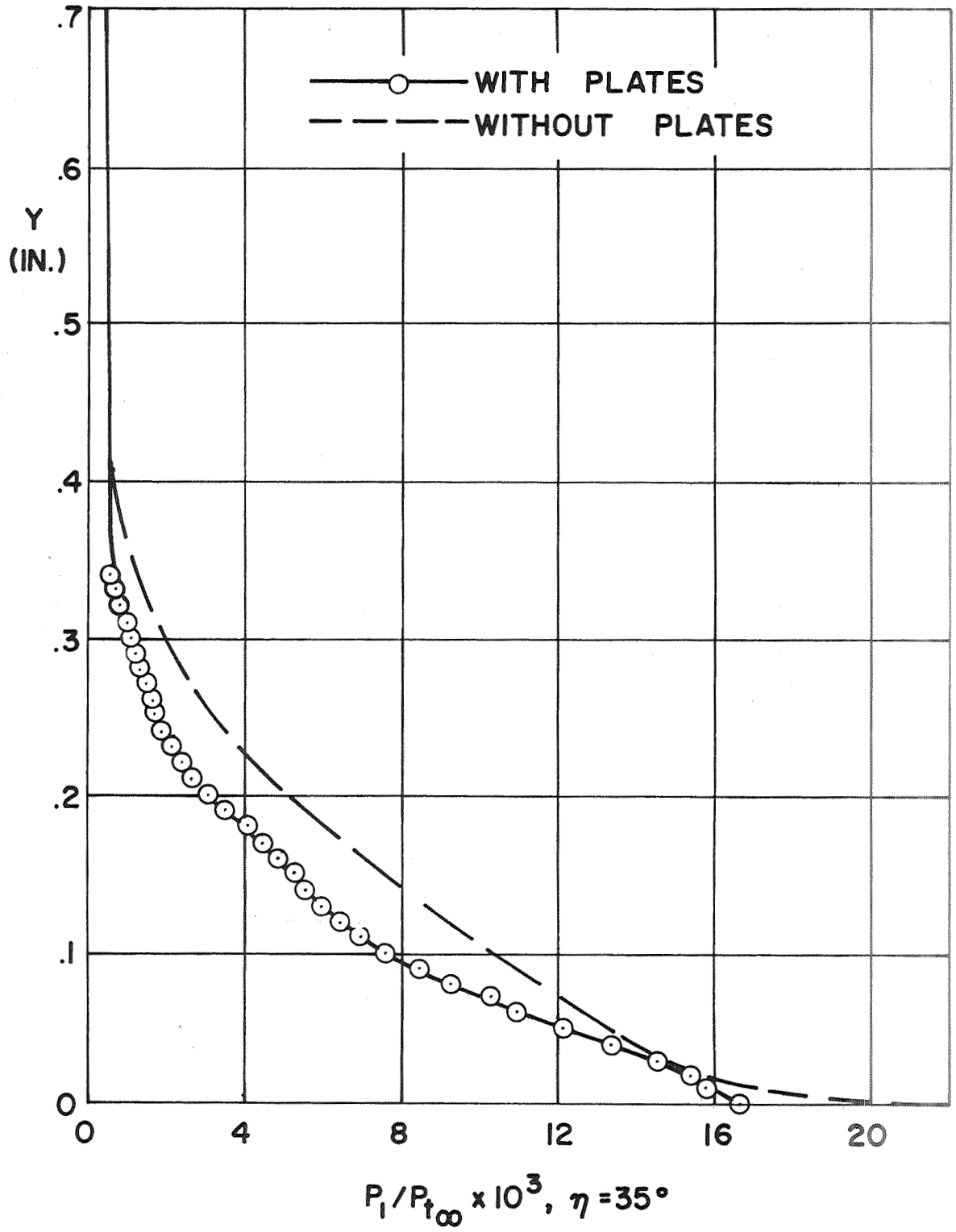

Fig. 12 Static Pressure Profile at $\eta = 35^{\circ}$

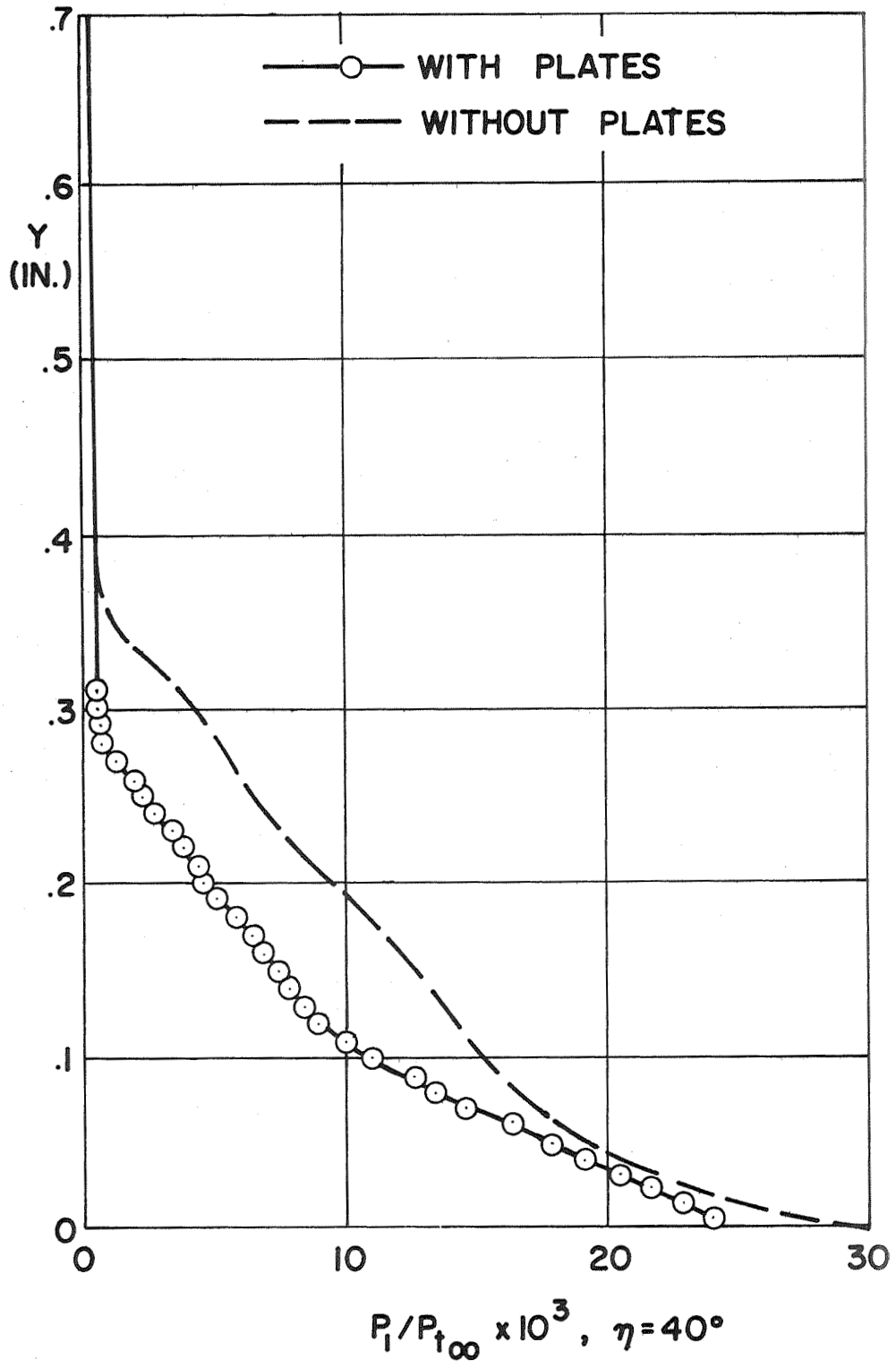

Fig. 13 Static Pressure Profile at $\eta = 40^{\circ}$

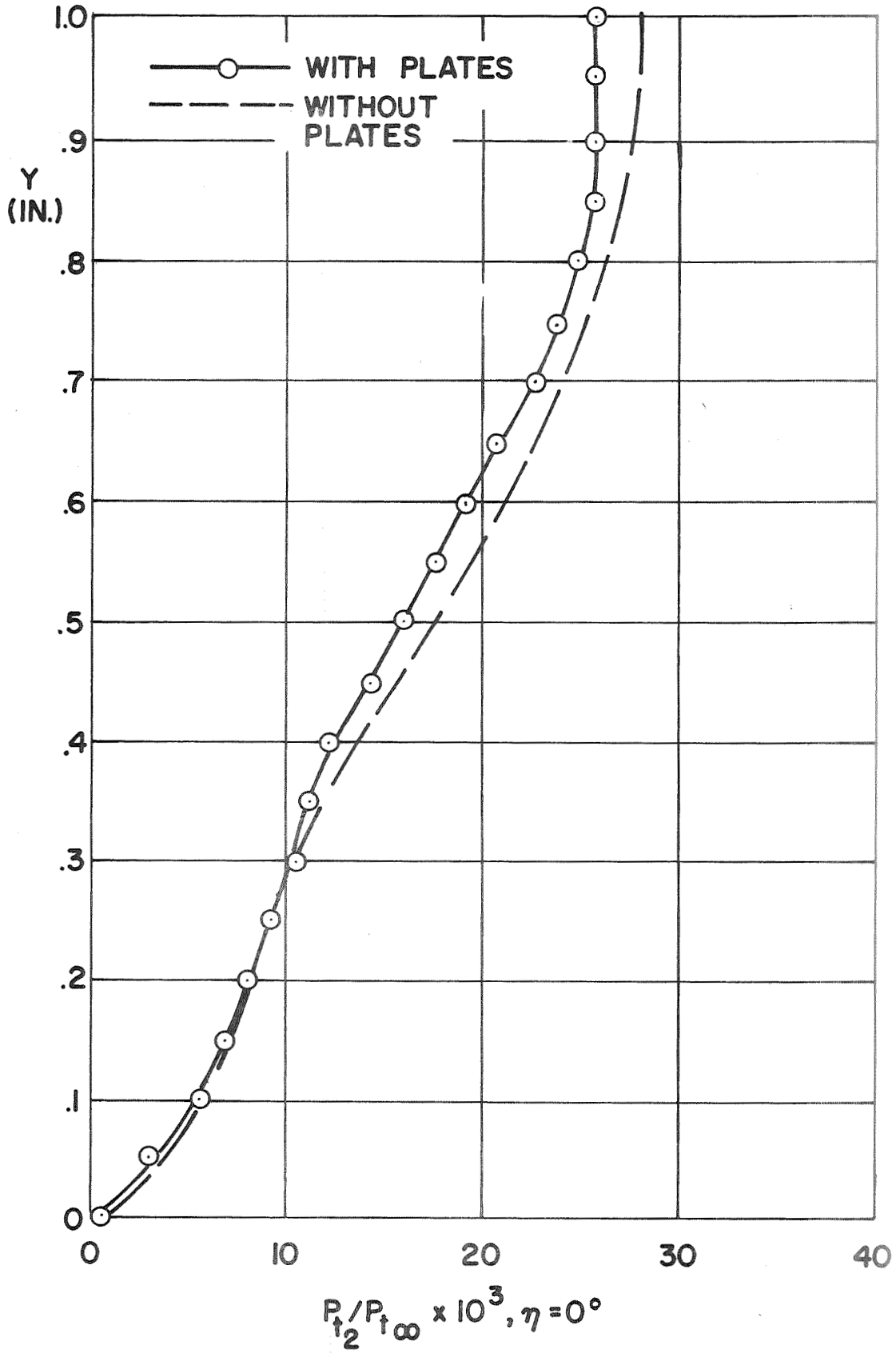

Fig. 14 Pitot Pressure Profile at $\eta = 0^\circ$

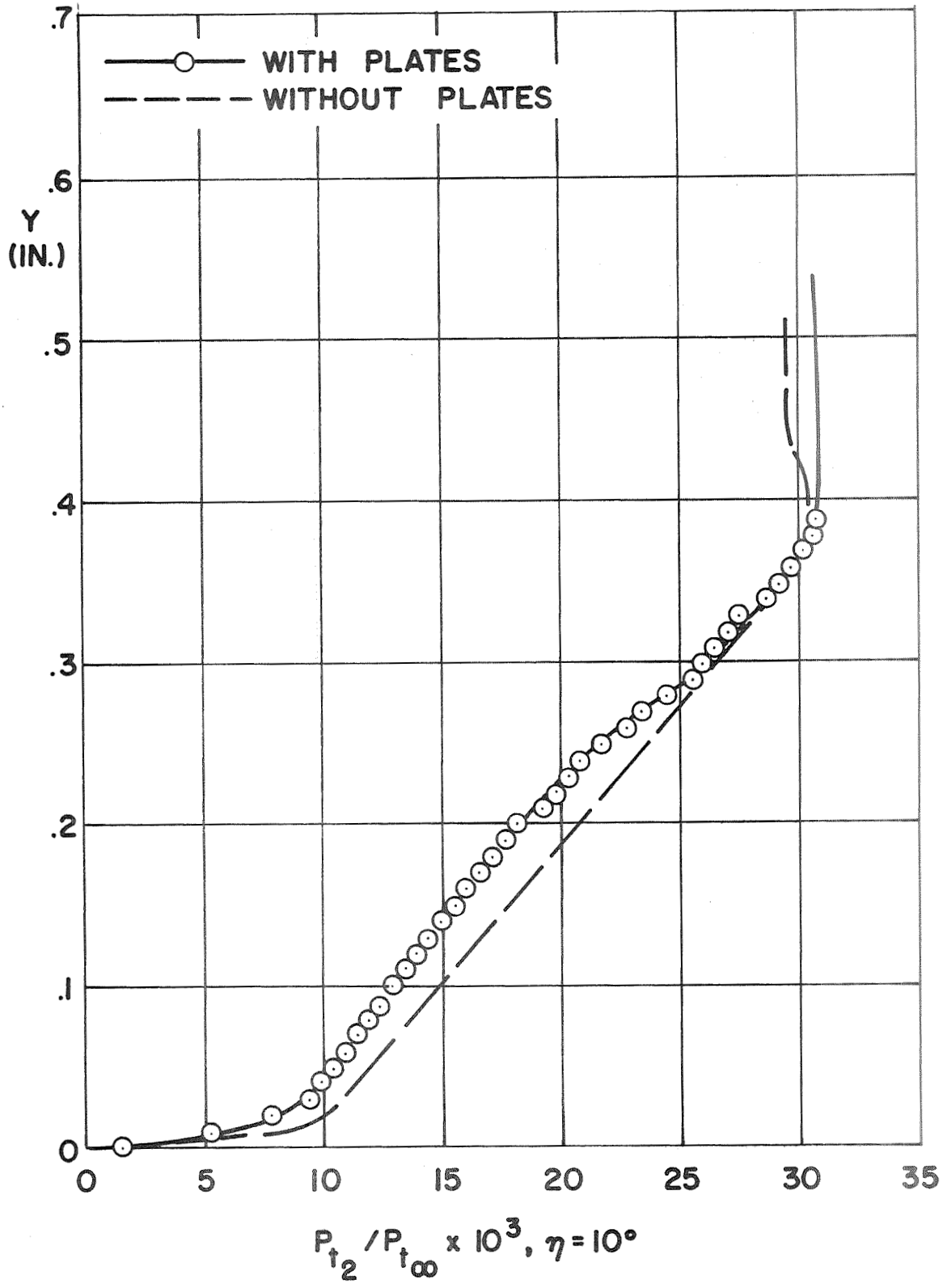

Fig. 15 Pitot Pressure Profile at $\eta = 10^{\circ}$

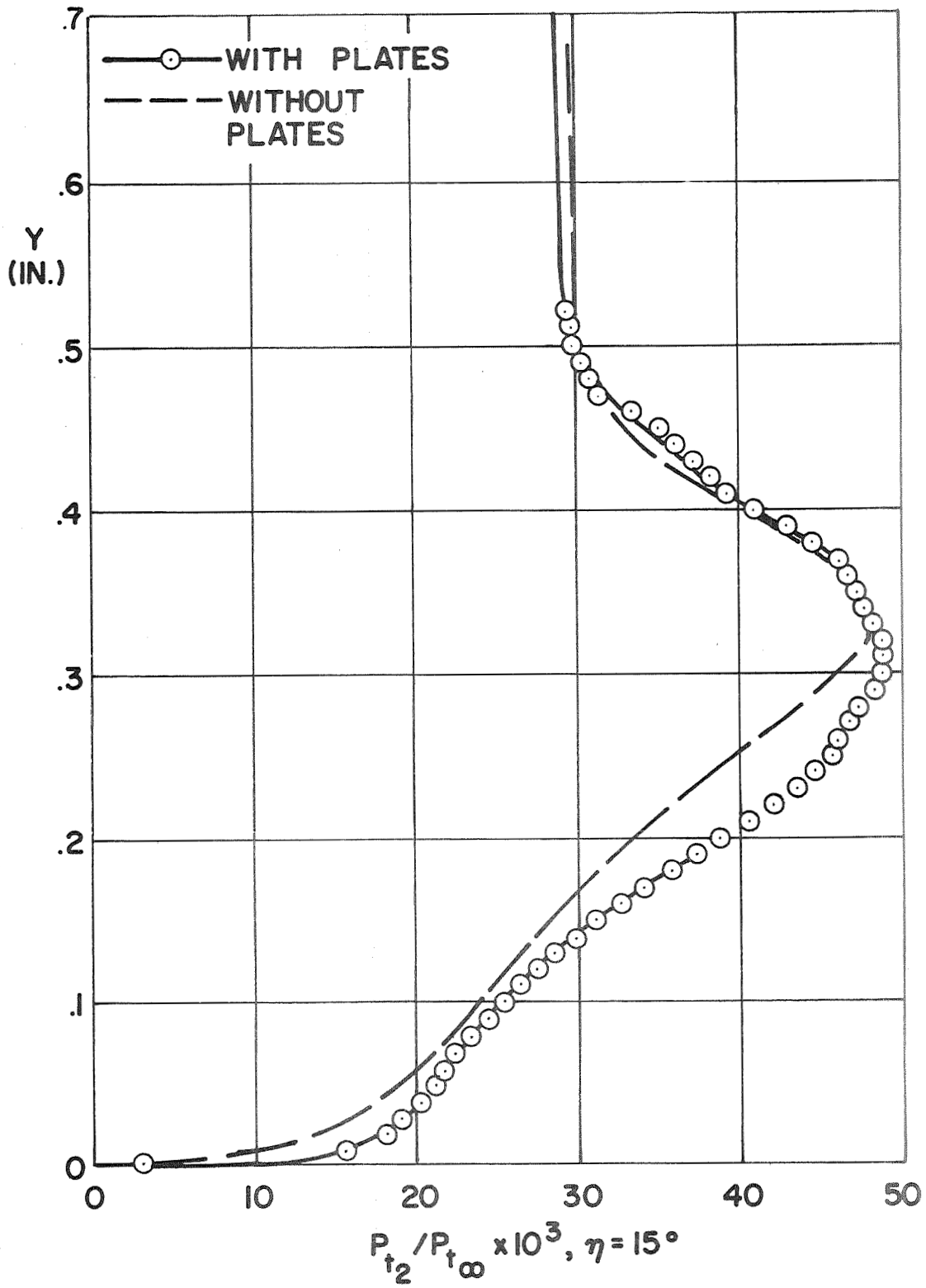

Fig. 16 Pitot Pressure Profile at $\eta = 15^{\circ}$

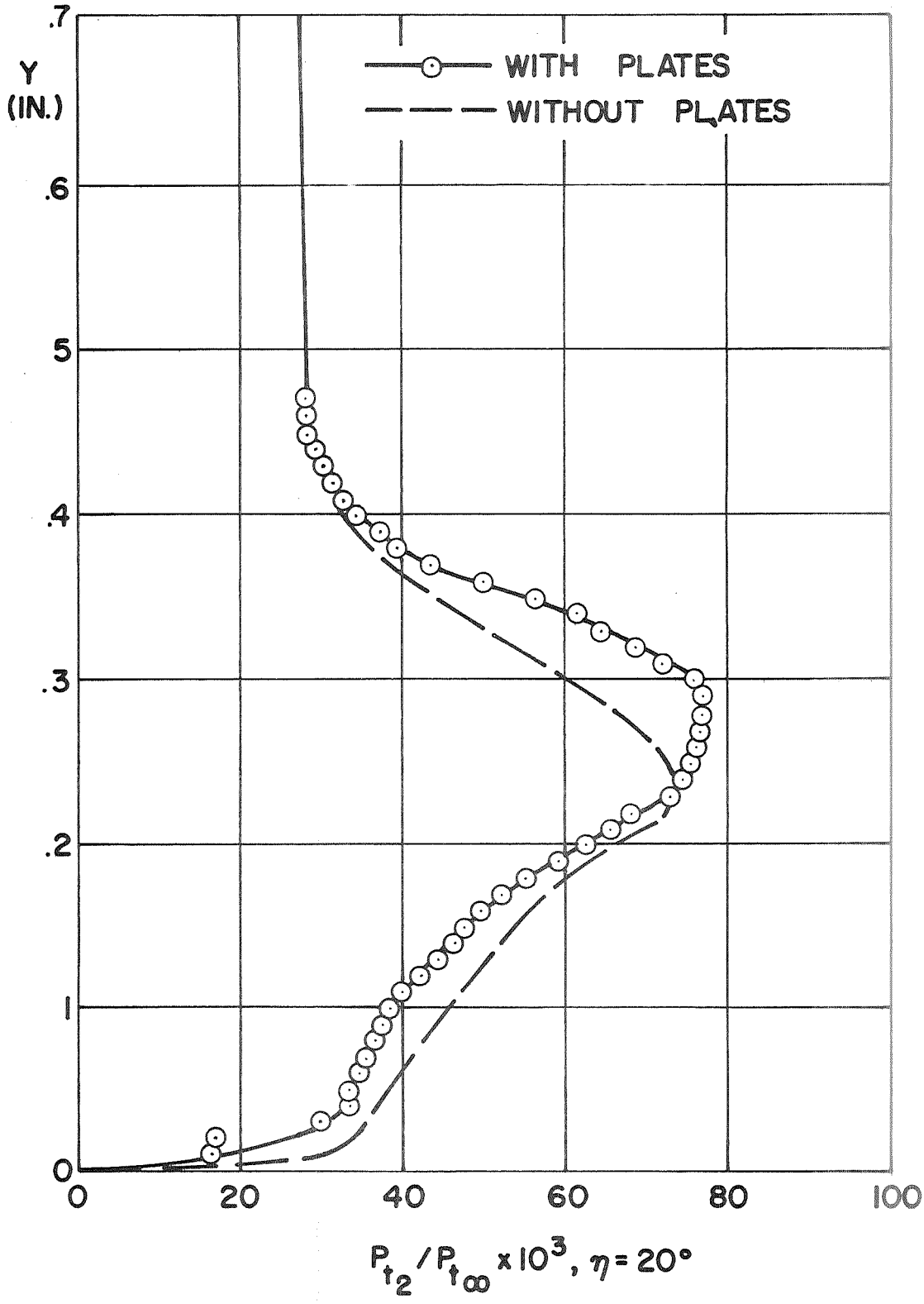

Fig. 17 Pitot Pressure Profile at $\eta = 20^{\circ}$

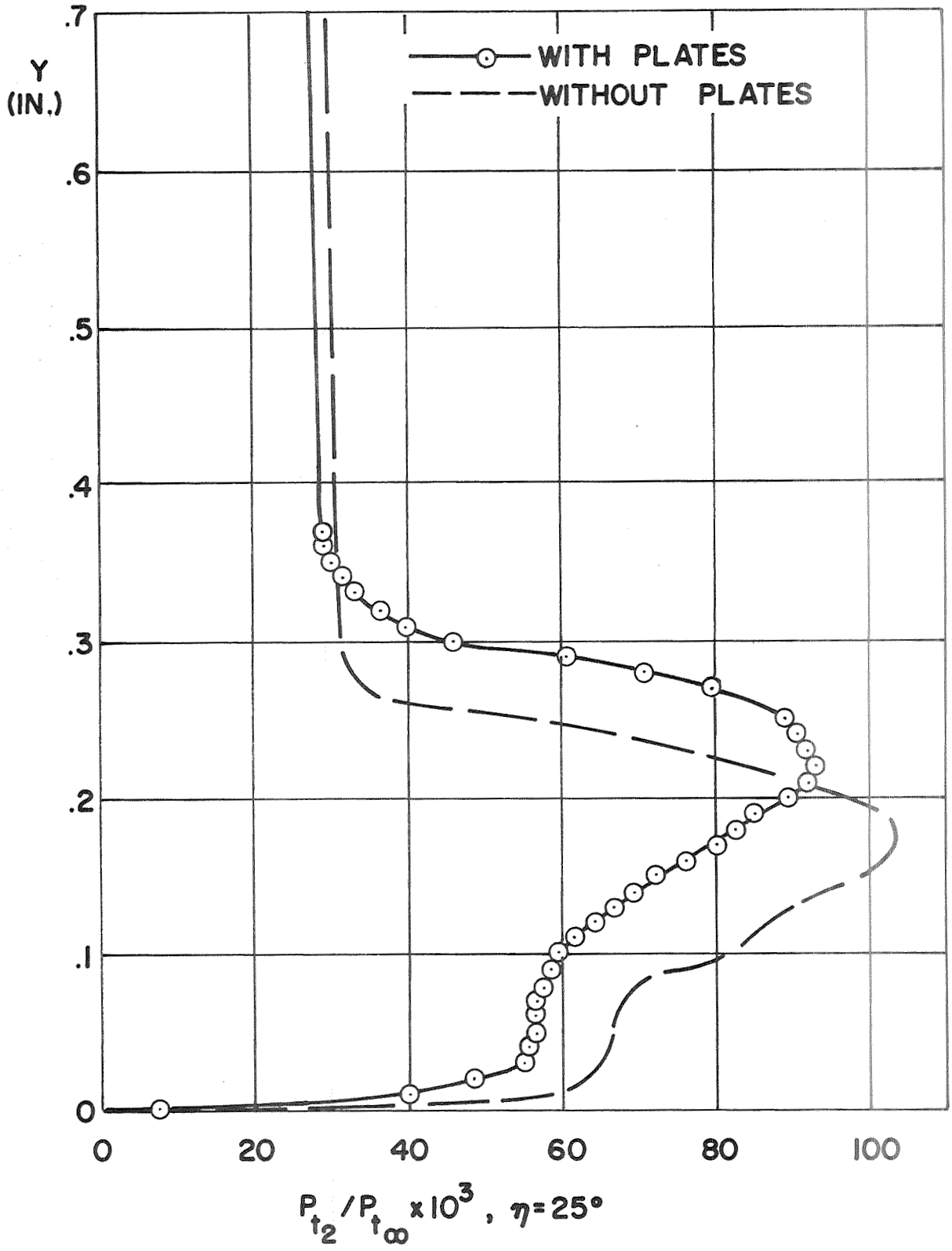

Fig. 18 Pitot Pressure Profile at $\eta = 25^\circ$

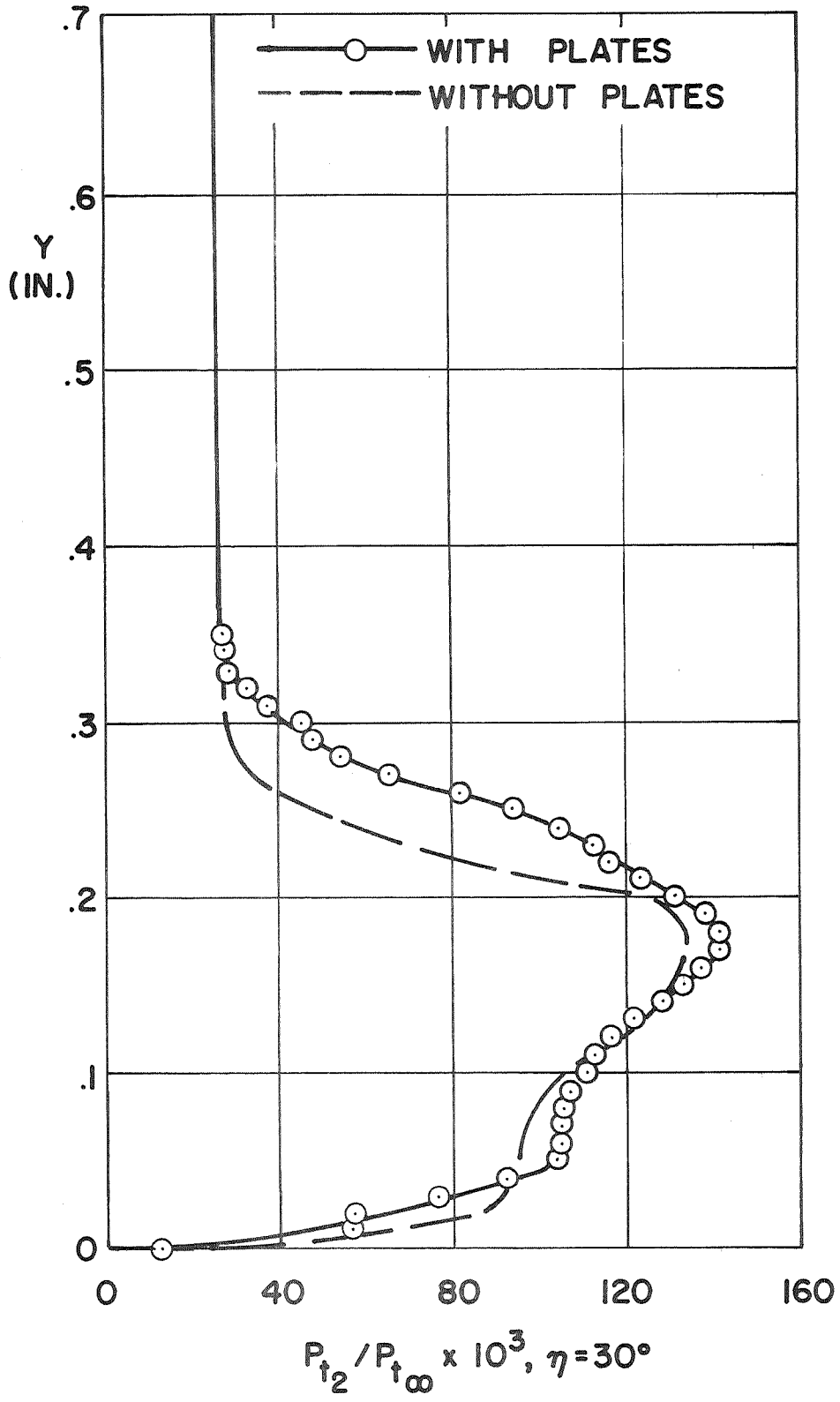

Fig. 19 Pitot Pressure Profile at $\eta = 30^\circ$

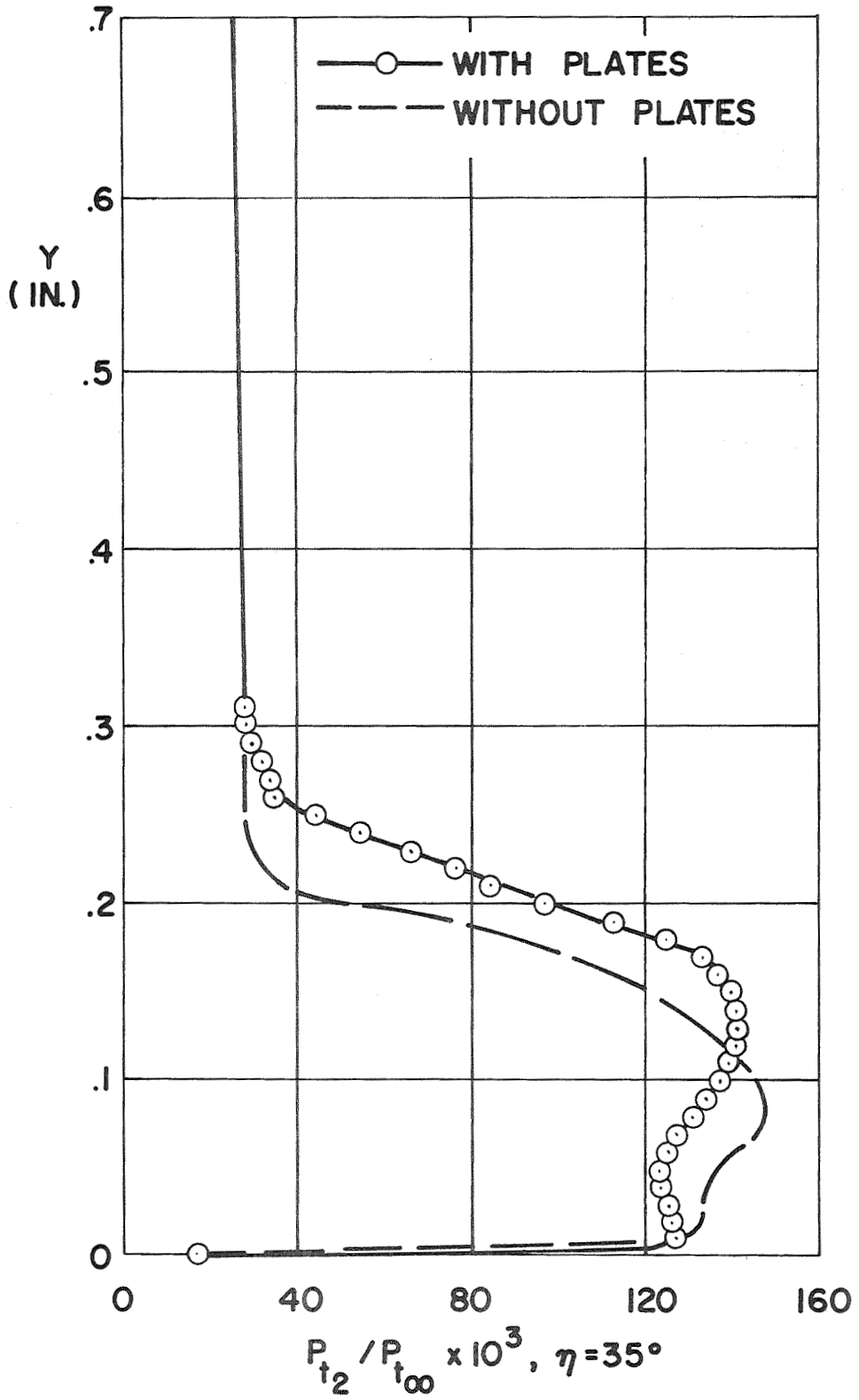

Fig. 20 Pitot Pressure Profile at $\eta = 35^\circ$

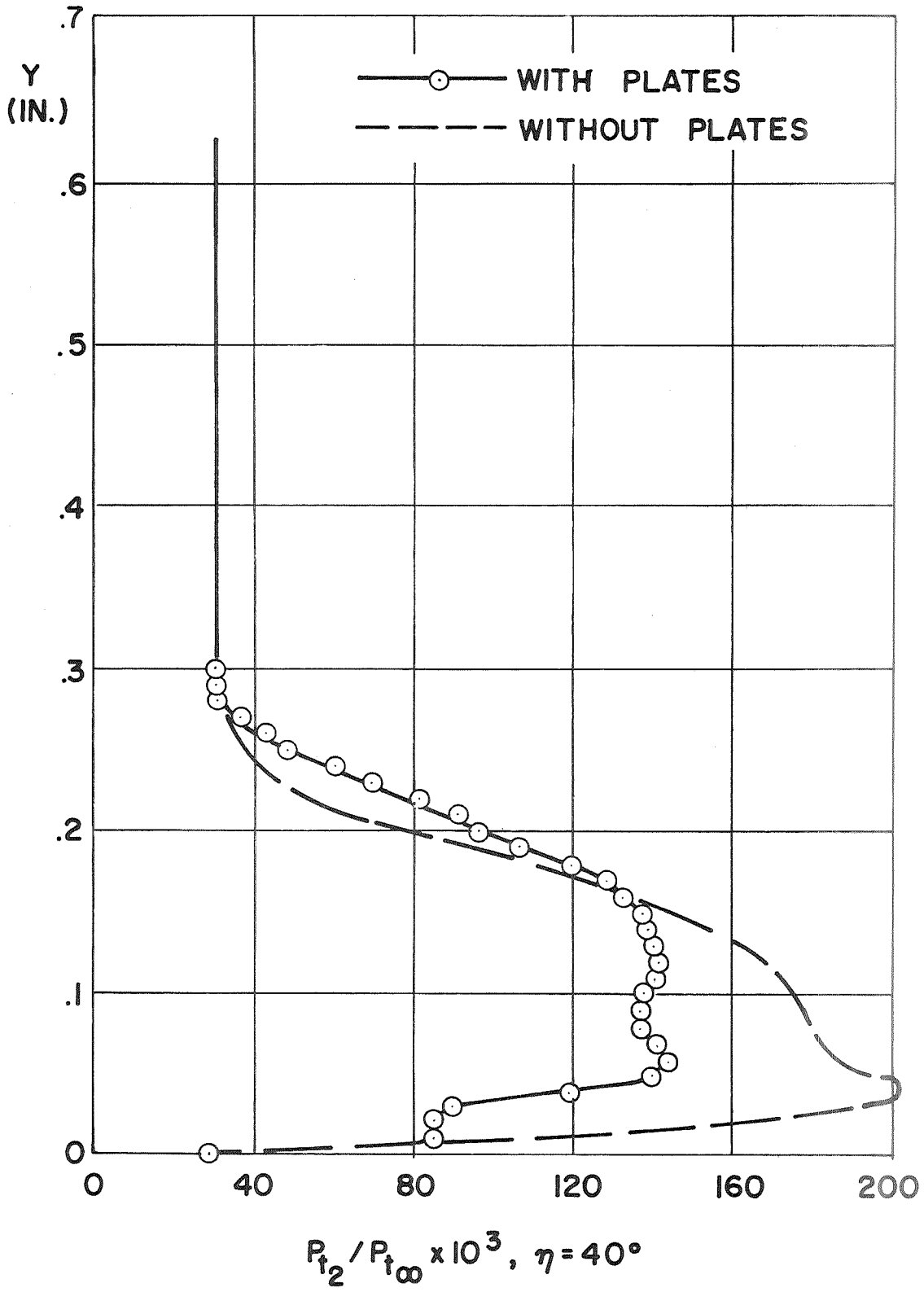

Fig. 21 Pitot Pressure Profile at $\eta = 40^\circ$

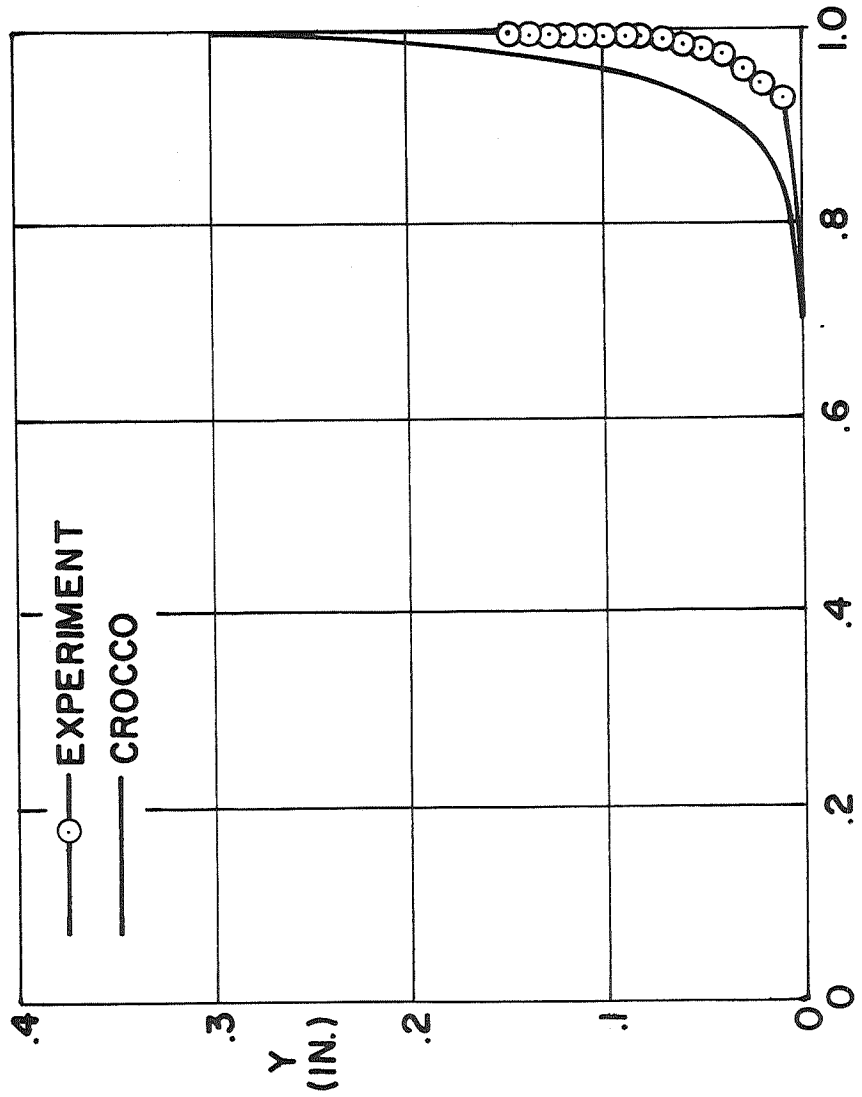

Fig. 22 Stagnation Temperature Profile at $\eta = 0^\circ$

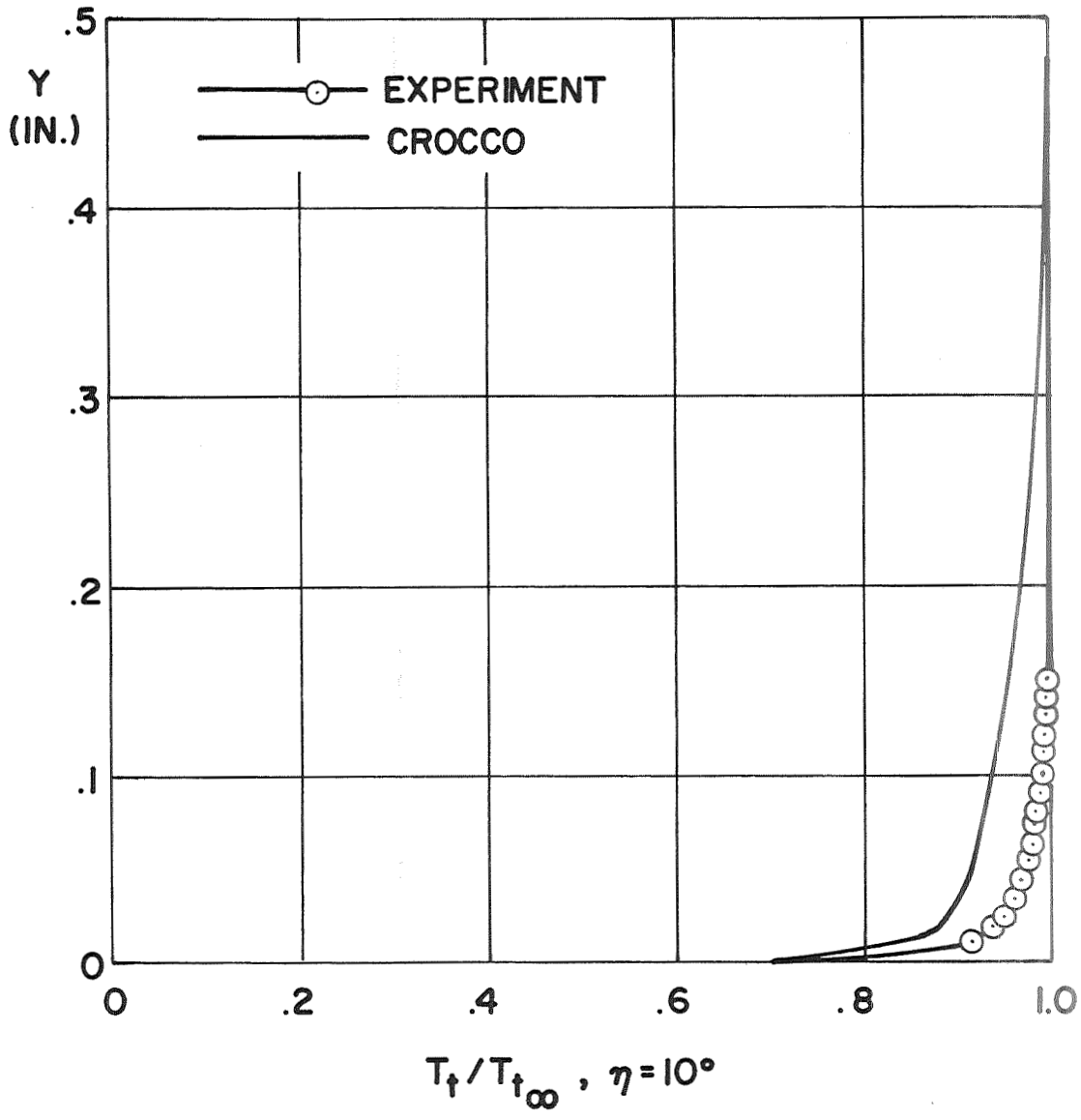

Fig. 23 Stagnation Temperature Profile at $\eta = 10^{\circ}$

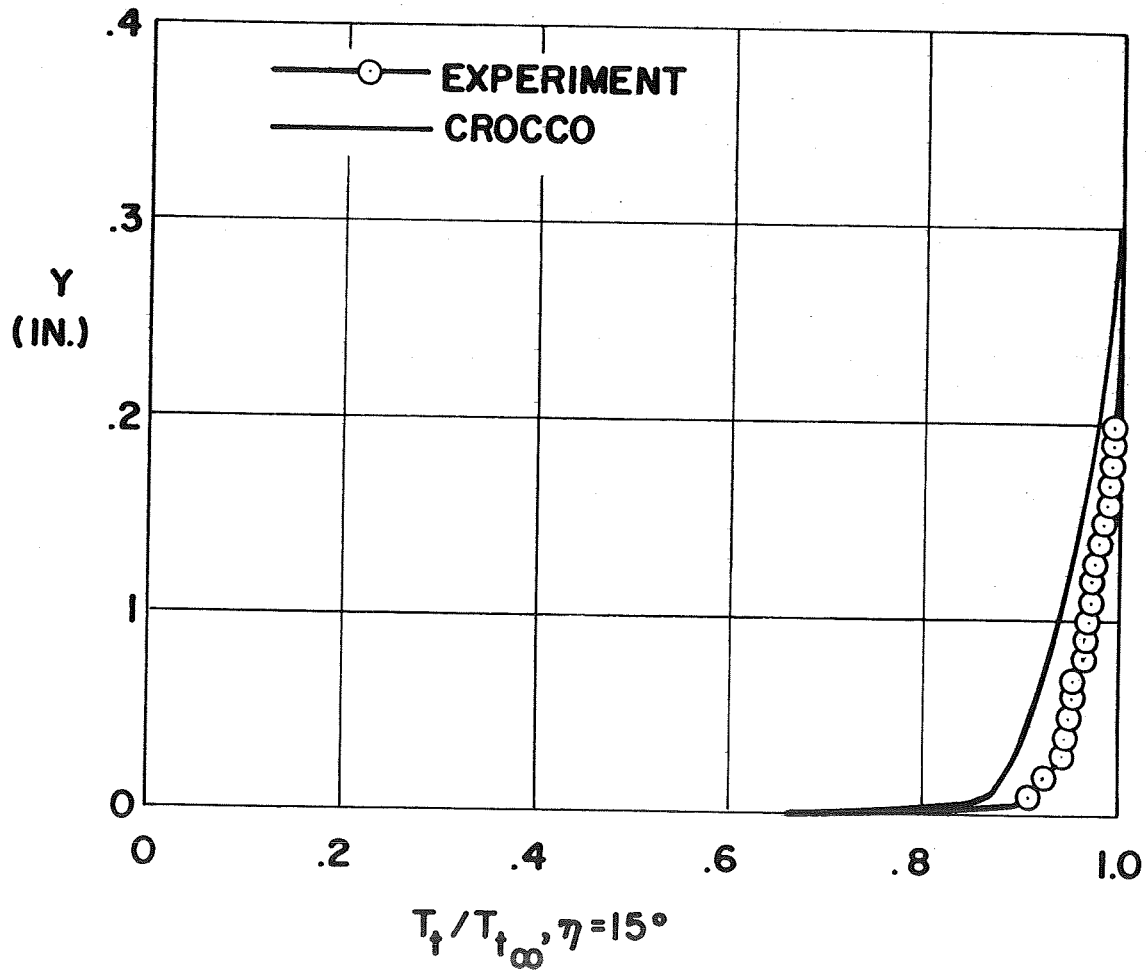

Fig. 24 Stagnation Temperature Profile at η = 15°

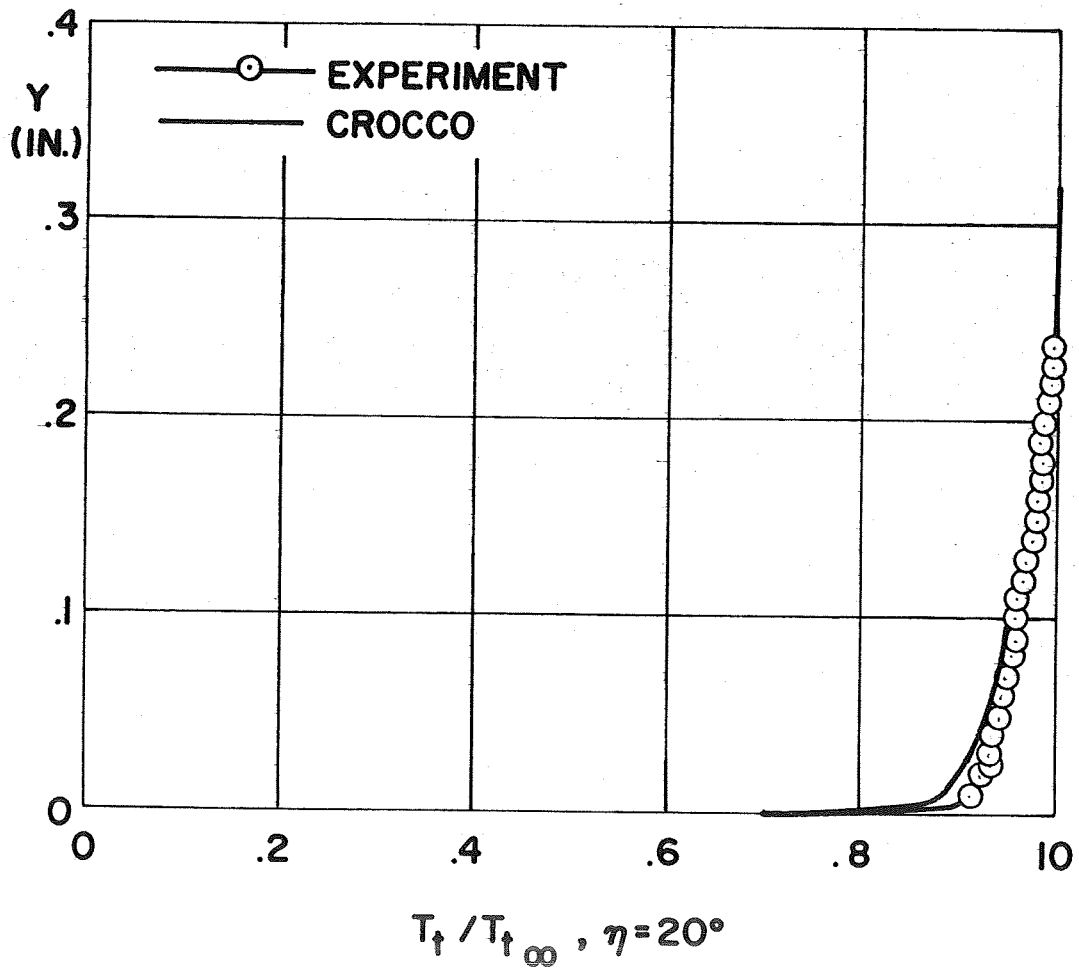

Fig. 25 Stagnation Temperature Profile at $\eta = 20^{o}$

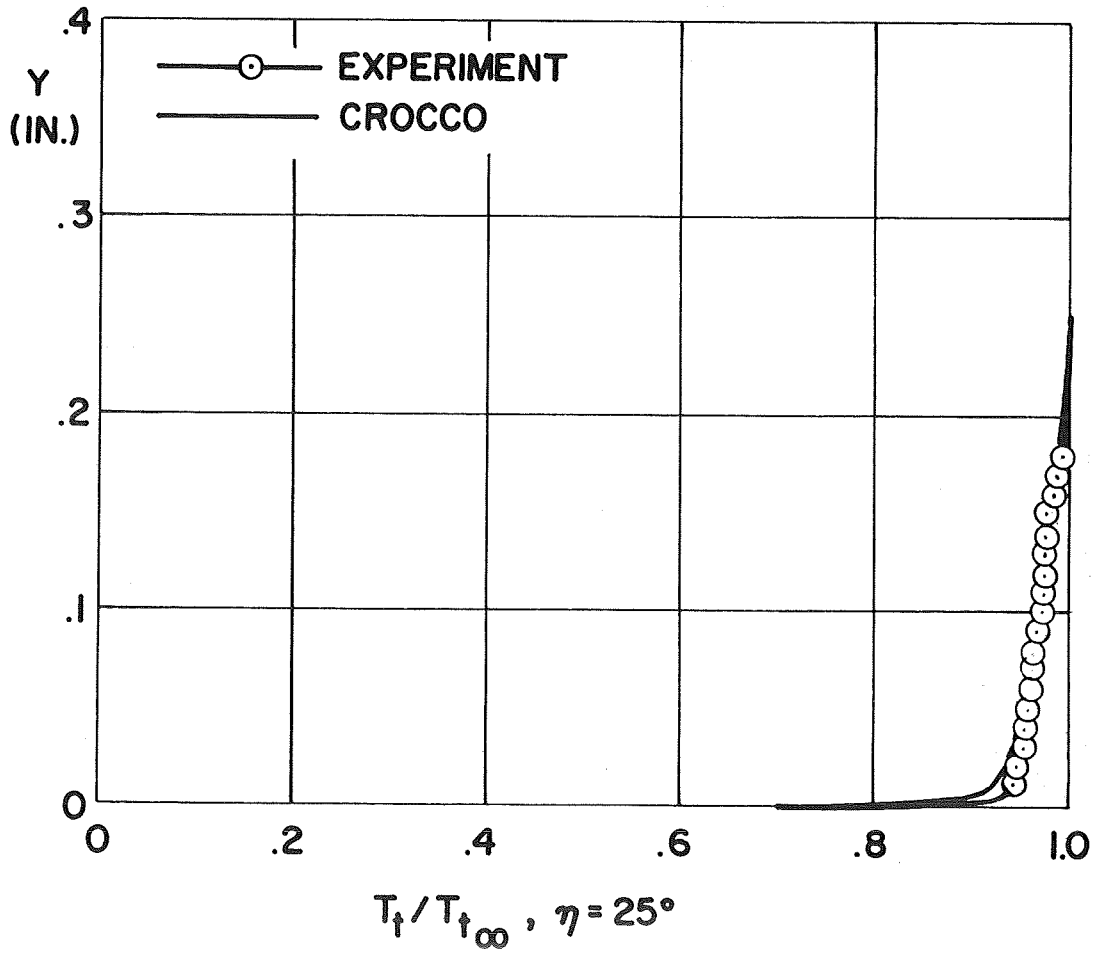

Fig. 26 Stagnation Temperature Profile at $\eta = 25^{\circ}$

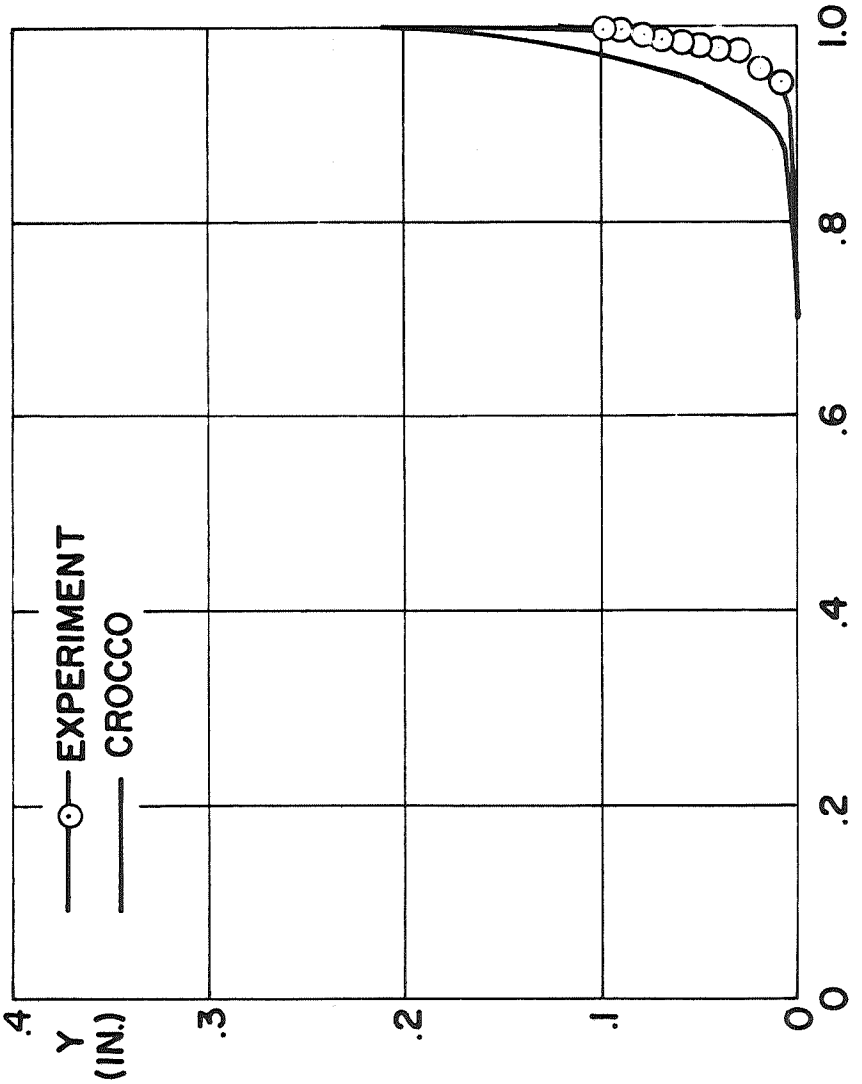

Fig. 27 Stagnation Temperature Profile at $\eta = 30^{\circ}$

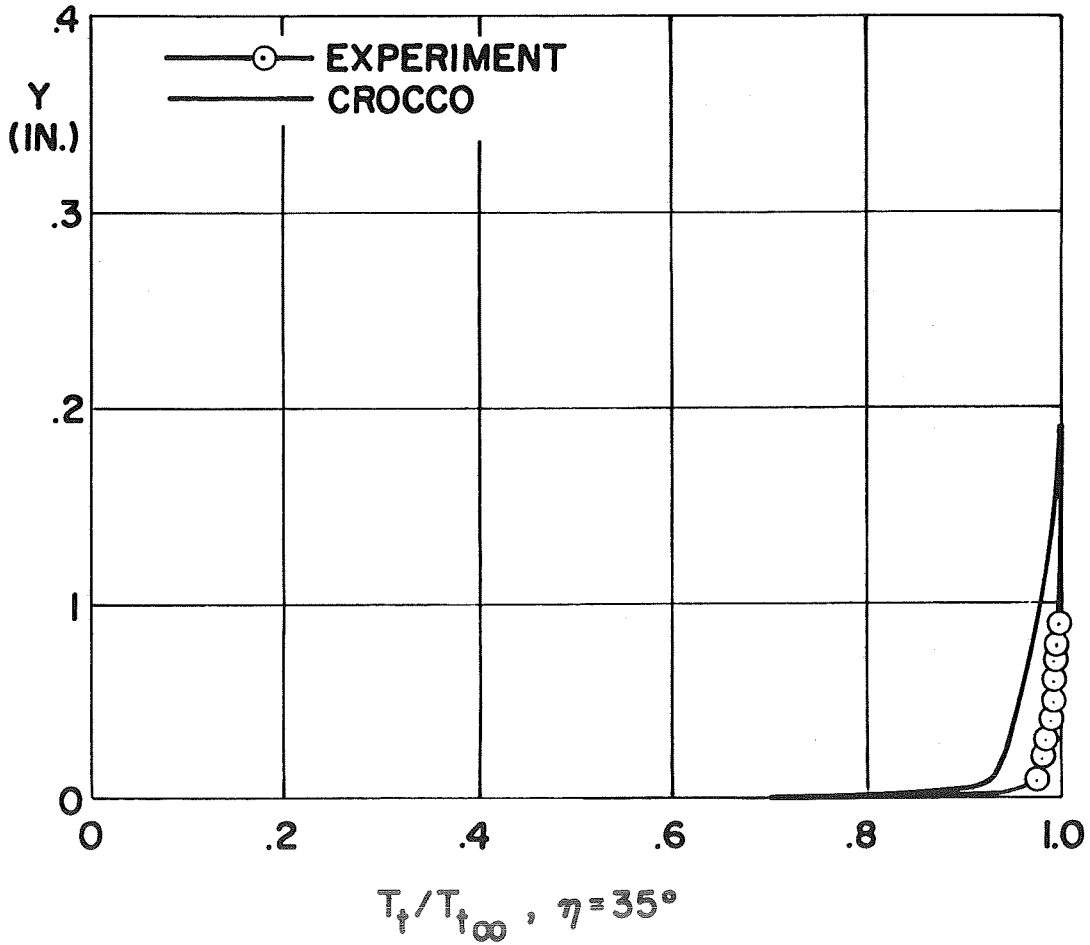

Fig. 28 Stagnation Temperature Profile at $\eta = 35^{o}$

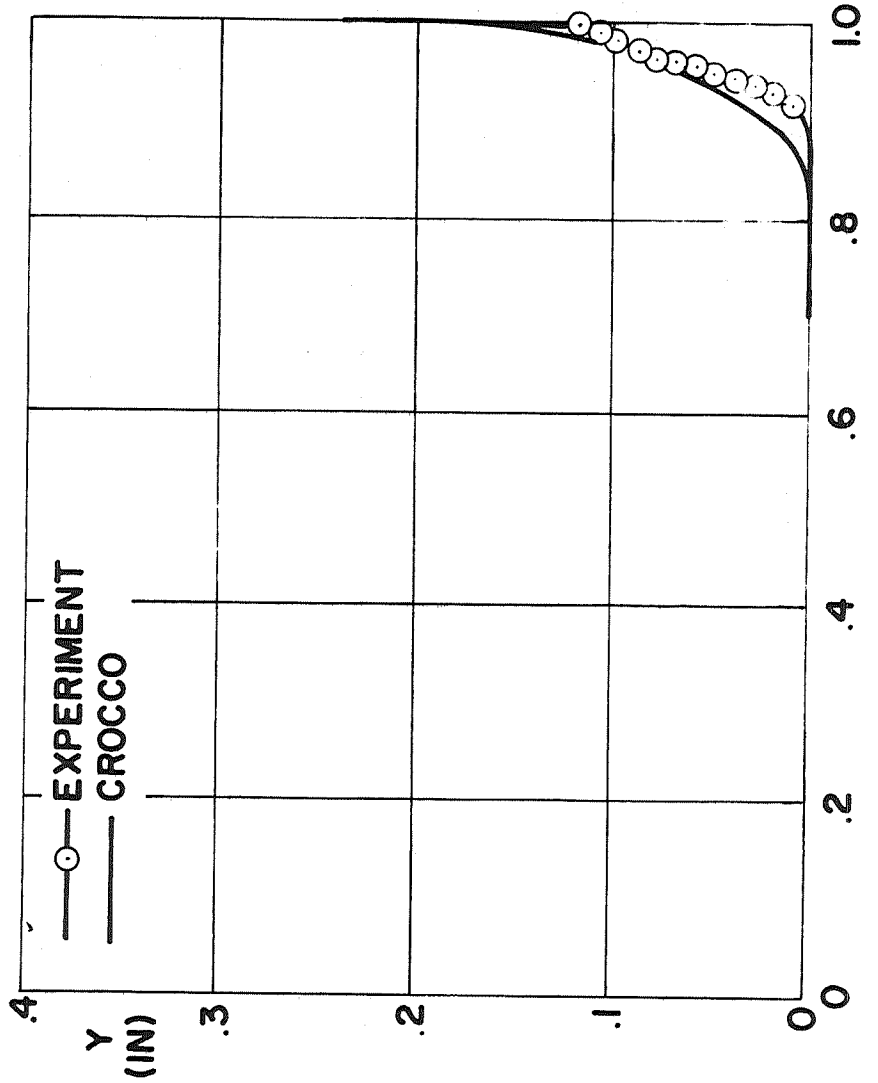

Fig. 29 Stagnation Temperature Profile at $\eta = 40^\circ$

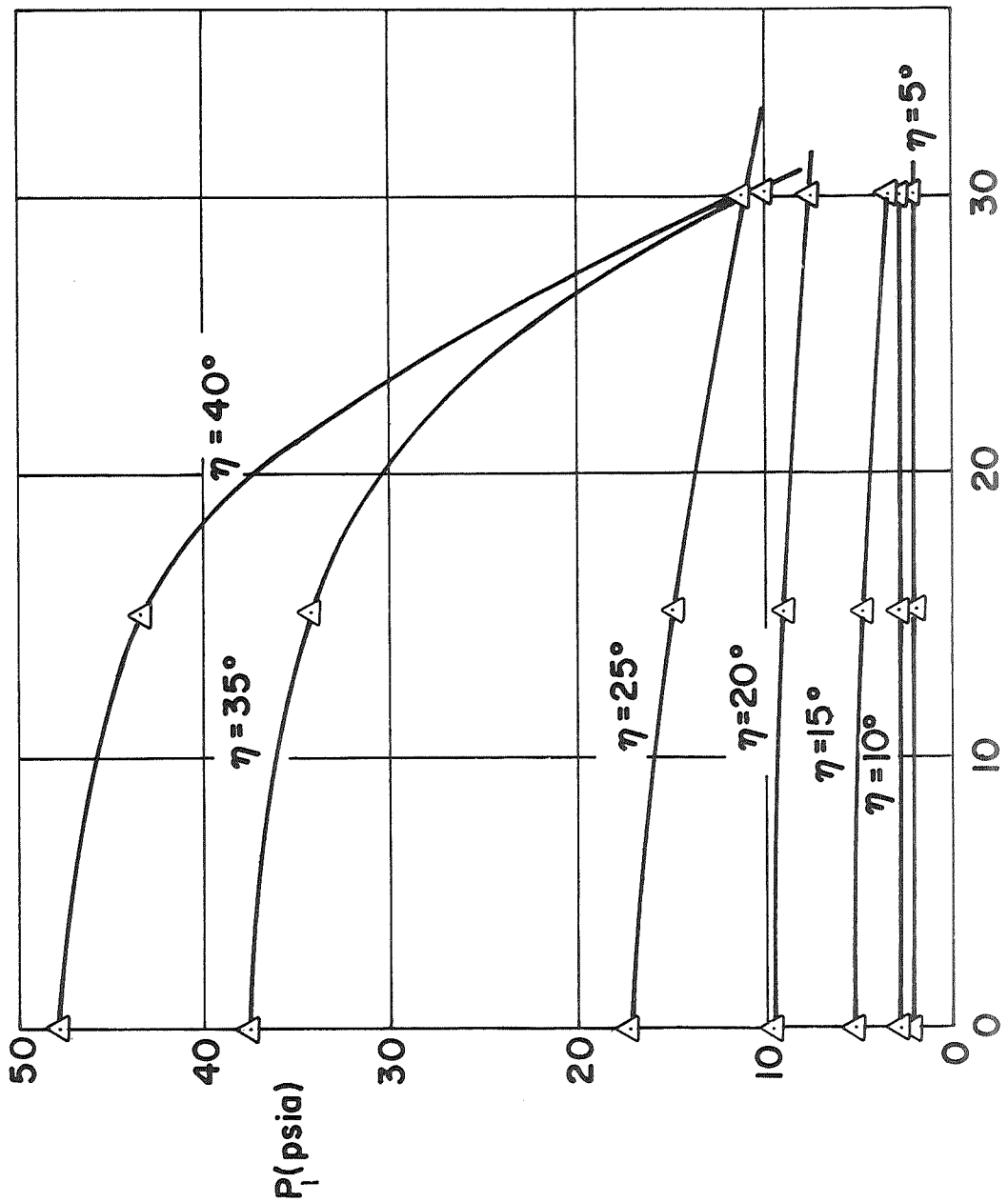

Fig. 30 Peripheral Static Pressure Distribution

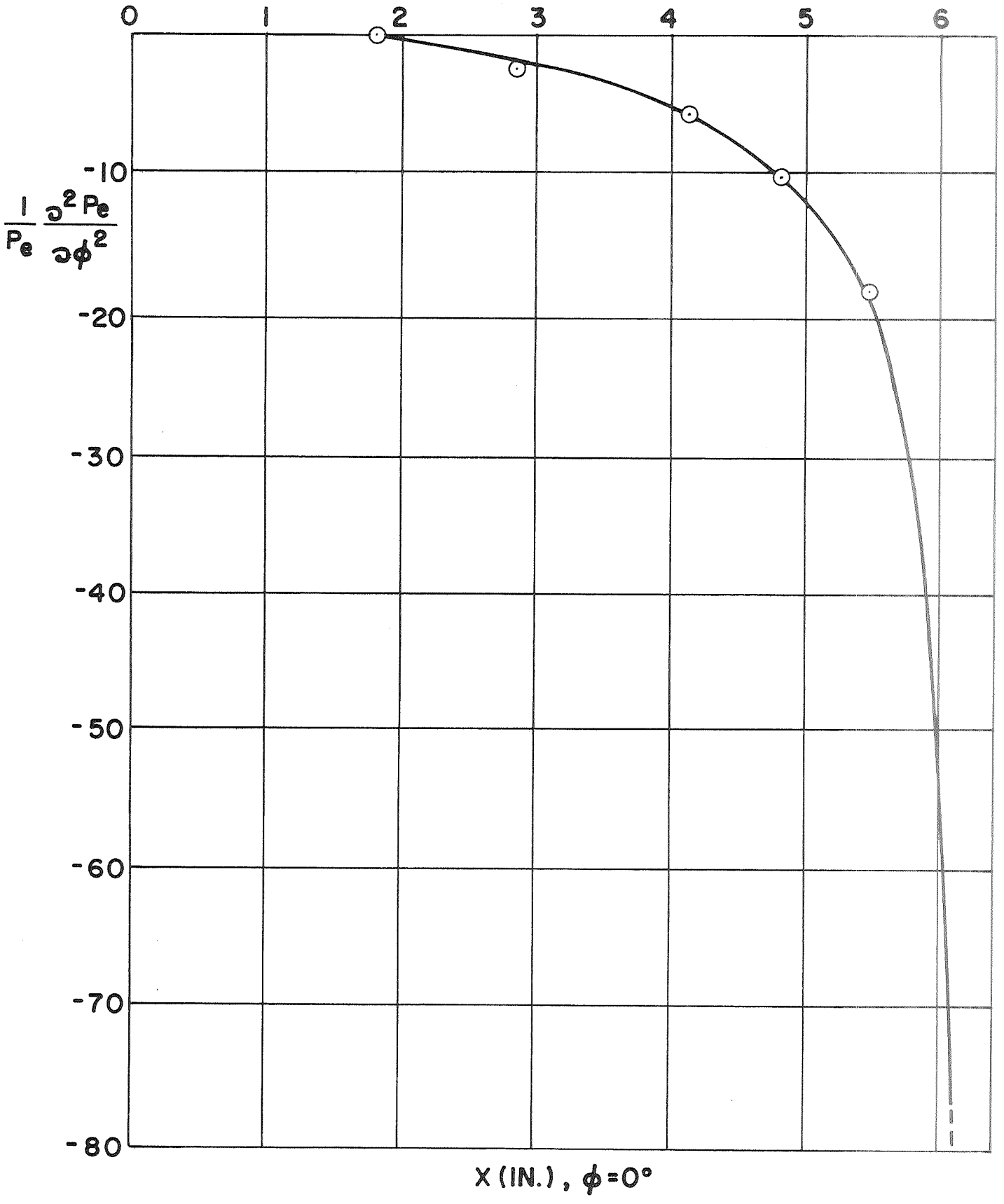

Fig. 31 Cross Flow Parameter Evaluated at the Meridian Plane

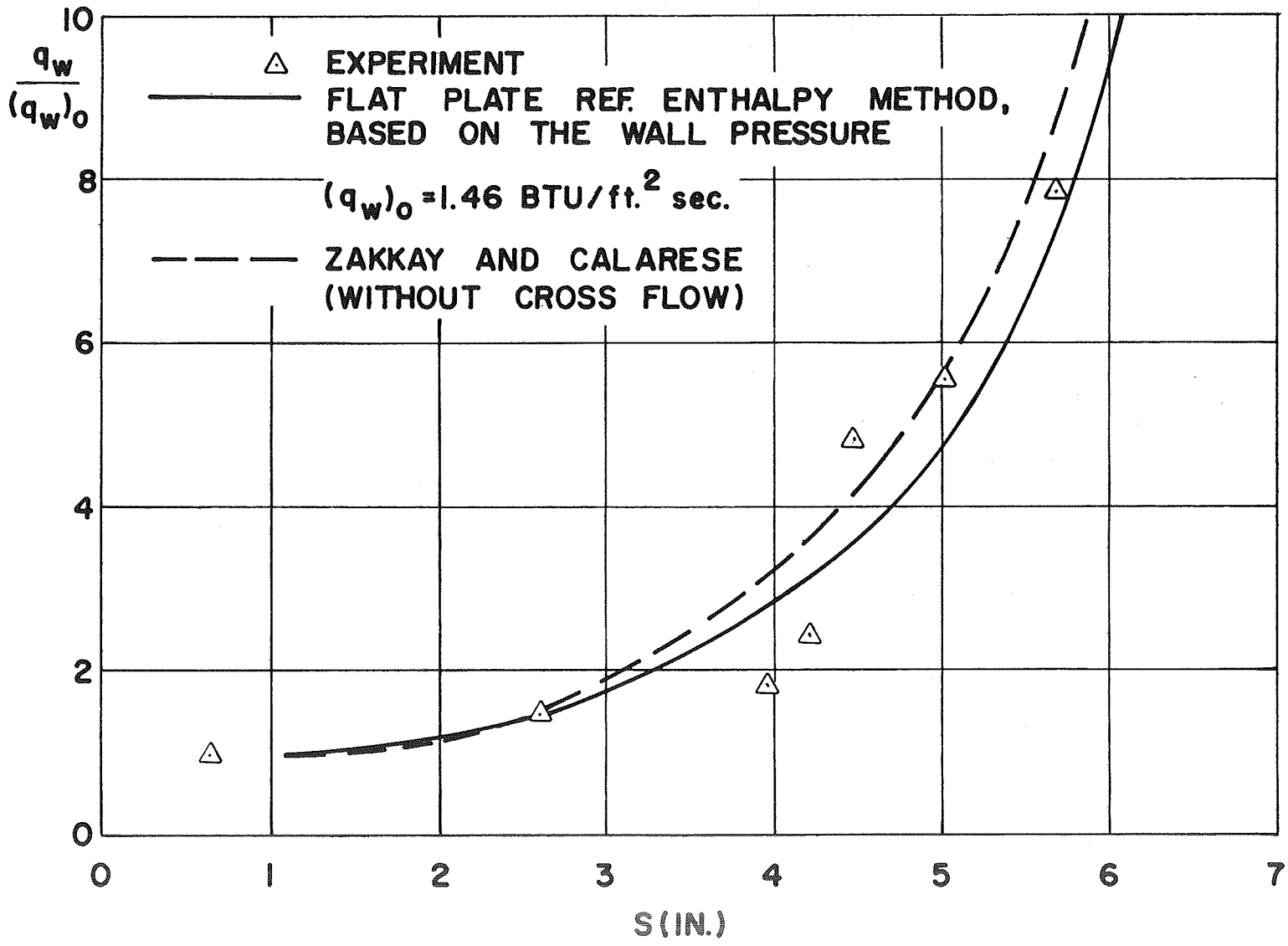

Fig. 32 Heat Transfer Rates without Cross Flow on Flared Surface